Modeling of Mechanical Behavior of Structural Masonry

By Mohammadreza Mohammadi, M.Sc.

A Thesis Submitted to the School of Graduate Studies in Partial Fulfillment of the Requirements for the Degree Master of Applied Science

McMaster University

MASTER OF APPLIED SCIENCE (2018) McMaster University
(Civil Engineering) Hamilton, Ontario

TITLE: Modeling of Mechanical Behaviour of Structural Masonry

AUTHOR: Mohammadreza Mohammadi
B.Sc. (Sharif University of Technology, Tehran, Iran)

SUPERVISOR: Professor. S.Pietruszczak

NUMBER OF PAGES: viii, 58

Abstract

Masonry is an orthotropic material that exhibits distinct directional properties due to the existence of mortar joints acting as planes of weakness. Therefore, a constitutive model employed in the numerical analysis should be capable of describing the anisotropic behavior. In this thesis, a comprehensive framework is outlined for modelling of the mechanical behaviour of structural masonry. In this framework, the anisotropic material properties are described using the microstructure tensor approach (Pietruszczak and Mroz, 2001).

First, a mathematical formulation defining the conditions at failure is discussed. The formulation contains several material parameters as well as material functions that describe the anisotropic behaviour. The identification procedure for these functions is outlined and is verified using the experimental tests conducted by Page (1983).

Later, an extensive numerical study, including a set of numerical simulations of biaxial compression-tension and biaxial compression tests for different orientations of bed joints, is conducted to verify the macroscopic failure criterion. The results are then compared with the experimental data of Page (1983).

In the last part of the thesis, some 3D finite element simulations of a shaking table test are performed involving a reduced scale model of four storey masonry building subjected to seismic excitation. A linear dynamic analysis, in which the proposed macroscopic failure criterion is incorporated through the UMAT subroutine, is carried out to assess the plastic admissibility of the stress field. The results including the distribution of the value of the failure function are then compared with the crack pattern in the experimental test.

Acknowledgement

Firstly, I would like to express my gratitude and deep appreciation to my supervisor, Professor S. Pietruszczak, for his continued support, guidance, and motivation throughout all the time of research and writing of this thesis. Without his support and encouragement, the completion of this research would have been impossible.

I would also like to thank Dr. Peijun Guo and Dr. Lydell Wiebe for their valuable comments on this thesis.

Special thanks are also expressed to my supervisor, Professor S. Pietruszczak, and the Department of Civil Engineering at McMaster University for their financial support. My sincere thanks also go to Dr. Amir Akhaveysi for his advice during the different parts of my research.

Finally, I must express my love and very profound gratitude to my parents, Ali and Mahnaz, and my sisters, Mohaddese, Yalda, and Mahya, for all their endless love, spiritual support, and sacrifices throughout my life. Without their dedications, I would never be in the position I am now.

Table of Contents

Table of Figures

List of Tables

Chapter 1

INTRODUCTION

1.1. Background

Masonry is one of the most common construction materials due to its various advantageous properties such as high durability, low maintenance cost, fire resistance, and design flexibility. However, nonlinear behavior of the structural masonry is a major drawback leading to many challenges in the design of the masonry structures. This nonlinear behavior is due to the complex composition of the masonry that comprises brick units as well as bed and head joints acting as planes of weakness. Therefore, many masonry structures have been designed based on the engineering intuition and experience rather than a rigorous analysis.

In recent years, many numerical studies have been conducted to model the mechanical behaviour of structural masonry. Two distinct approaches have been followed for the numerical simulations of masonry structures: meso-modelling and macro-modelling. In meso-modelling approach, the individual components, i.e. units and mortar joints, are simulated by continuum elements and the unit-mortar interfaces are considered as discontinuous elements. On the other

hand, in the macro-modelling approach, the units, mortar and unit-mortar interfaces are smeared out in a representative volume element describing the macroscopic behaviour of the masonry.

The main aim of this research is to develop a macroscopic failure criterion for the masonry brickwork, which can be directly incorporated in the numerical analysis of masonry structures.

1.2. Literature Review

The previous studies on structural masonry can be divided into two broad categories: experimental testing and numerical modelling. Over the past few decades, several experimental tests on brick masonry were conducted in order to provide information assisting in the design of the masonry structures. The experimental investigations have been performed at the material level as well as macroscopic level. The former involve assessment of conditions at failure in masonry constituents, including brick and mortar. Atkinson et al. (1985) and Bierwirth et al. (1993) used a linear form of the failure envelope for mortar. They also proposed a polynomial curve as the failure envelope for brick units in the tension-compression regime based on the results of biaxial tests. In addition, the strength parameters of brick units and mortar have been determined by conducting a series of uniaxial tension and compression tests. Also, the shear characteristics of the interface were identified by Atkinson et al. (1989) for studying the brickwork behavior under cyclic loadings.

The first experimental study on the mechanical behavior of brick masonry at the macroscale was performed by Samarasinghe and Hendry (1982). The authors examined a number of scaled brickwork panels under a uniform biaxial tension-compression loading. They also suggested a failure envelope which depends on the principal stresses and the orientation of the bedding planes. The most comprehensive research yet on macroscopic behaviour of masonry was that performed

by Page (1981,1983). In those studies, a set of biaxial compression-tension and biaxial compression tests were carried out to define the failure surface for different orientations of bed joints. Drysdale and Khattab (1995) conducted similar research on the behaviour of grouted concrete masonry, in which the specimens were tested under biaxial tension-compression loading. Their study also indicated a strong dependency of the failure modes, strength parameters, and the deformation characteristics on both the orientation of bed joints and the principal stress ratio. In general, all the experimental tests mentioned above provided valuable data to establish various empirical design methods for masonry structures.

Numerical modelling of masonry structures is another category of research which attracted a great deal of attention in recent years. As stated before, the numerical modeling can be performed at meso- and macro-levels. In the former approach, the masonry constituents, i.e. the brick units and mortar joints, are modeled separately by different types of elements. The masonry units are represented by continuum elements, and discontinuous elements are used for modeling the mortar joints. The behavior of mortar joints has been described by various models such as discrete crack model, Coulomb friction model, combined Coulomb friction/tension cut-off/compression cap model or a user defined constitutive model; while an elastic or viscoelastic models have been typically used to describe the brick units. In these approaches, it was commonly assumed that the cracks occur in the mortar joints while the units remain intact. Page (1978) was perhaps the first one to conduct the finite element analysis of masonry brickwork. In his simulations, brick units were modeled by isotropic, elastic 2D elements, and the behavior of interface was described in terms of a brittle response in the tension regime and a bi-linear failure surface in compressive regime (τ-σ space). A similar numerical methodology was later employed by Lourenco and Rots (1993), who used continuum elements for brick units and zero-thickness interface elements for the

mortar joints. Their model was more advanced in terms of its ability to capture various failure mechanisms of the brick masonry. This was accomplished by defining a constitutive relation for the interface elements that accounted for joint tensile cracking and joint slipping, as well as using vertical interface elements inside the brick units to take into account the direct tension crack in the brick, as shown in Figure 1.1 (Lourenco et al. 1994 ;Lourenco & Rots, 1997) .

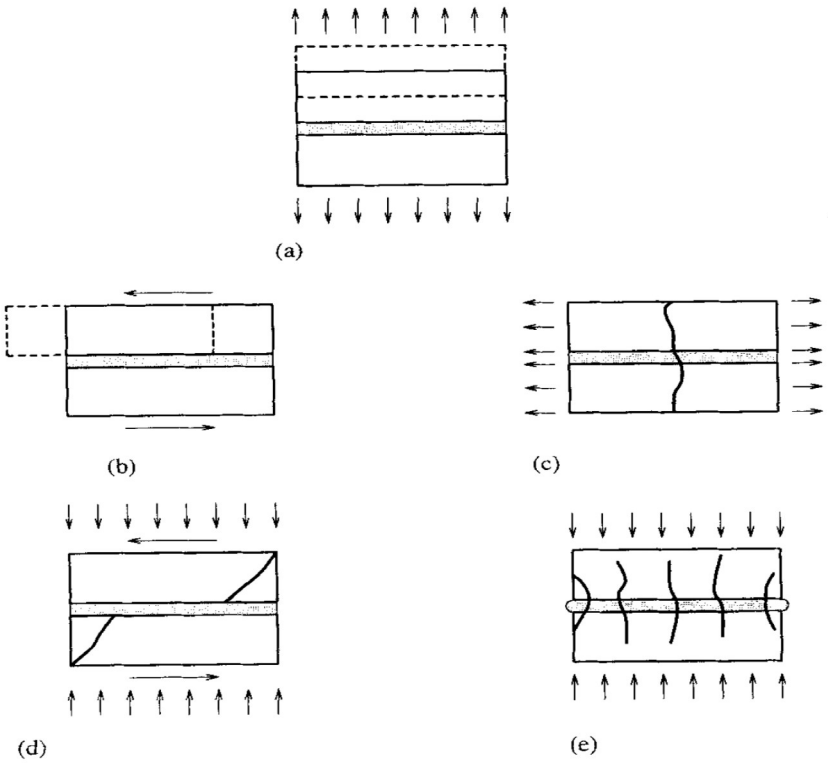

Figure 1.1 Failure Mechanisms of Masonry: (a) Joint Tensile Cracking (b) Joint Slipping (c) Direct Tension Crack in Brick Unit (d) Diagonal Tension Crack in Brick Unit (e) Masonry Crushing (Lourenço and Rots, 1997)

One of the main limitations of the stated approach is its inability to capture the mortar joints and brick interaction and to properly model the out-of-plane properties of masonry. Another important limitation is the lack of numerical efficiency. In other words, this methodology would not be feasible for application to real engineering structures due to high computational time.

In vew of the mentioned limitations of the meso-modeling approach, the macroscopic numerical methodology should be used for modeling the mechanical behavior of masonry structures. In this framework, a representative element volume, in which the masonry constituents are smeared out using homogenization techniques, is introduced to describe the masonry material at macroscale. The average properties of the representative elementary volume are determined at the micro-level taking the geometric arrangement of the constituents into account. In recent years, many studies have been conducted to estimate the average properties of masonry brickwork. Micropolar Cosserat continuum models and the use of homogenization theory for periodic media are the main proposed approaches to address this problem. The Micropolar Cosserat continuum approach (e.g., Sulem and Muhlhaus, 1997; Masiani and Trovalusci, 1996) incorporates the Cosserat theory of elasticity or micropolar elasticity in which additional kinematic degrees of freedom, represented by the microrotation, are introduced to describe the rotations of single masonry units. Consequently, the stress tensor becomes non-symmetric due to adding the couple stress components. The Cosserat approach cannot be easily implemented to solve the engineering problems mainly because of difficulties with identification of material parameters associated with specification of rotational degrees of freedom.

The application of homogenization theory for the periodic media in determining the equivalent properties of brick masonry has been discussed in many studies. This approach has been adopted by Pande et al. (1989) and Pietruszczak & Niu (1992). In the former reference, a stacked brick-mortar system was considered which consisted of a set of parallel layers. In this approach, the equivalent elastic properties of brick masonry were assessed based on the elastic properties of brick and mortar. Later, this approach was improved by considering the masonry brickwork as consisting of sets of bed and head joints. The equivalent homogeneous orthotropic elastic

properties were then determined based on the elastic properties of brick and mortar and the thickness of the joints. Pietruszczak & Niu (1992) presented a two-step homogenization approach in which the brick masonry element is regarded as a structured medium. This medium consists of the brick matrix intercepted by two orthogonal sets of joints; bed joints forming continuous horizontal weakness planes, and head joints acting as aligned discontinuous weak inclusions. In the proposed homogenization approach the influence of the head and bed joints was considered separately in two successive stages to determine the equivalent properties of the structural masonry element. Also, a nonlinear average elastoplastic constitutive relation was proposed for the composite system using structural matrices which describe the macroscopic behaviour of the system as a function of the mechanical properties of the brickwork constituents, i.e. brick and mortar, and their volume contributions. Subsequently, the average elastic properties of the composite were also determined using the proposed constitutive relation. For an elastic material, there have been a number of other studies in which more accurate representations have been proposed using numerical homogenization (Anthoine (1995, 1997), Piszczek et al.(2001), Ma et al. (2001)). For instance, Anthoine (1995,1997) implemented the homogenization theory in a rigorous way to take into account the thickness of masonry. In that research, three types of problems, i.e. plane stress, plane strain, and generalized 3D, have been solved for the case of a running bond masonry, which was analyzed at the level of a basic cell using the finite element technique. This study indicated that the elastic characteristics of masonry are only slightly affected by the approximations of plane stress vs. general plane strain. However, use of the above approximations in the nonlinear range (plastic or damage) can lead to entirely different results. In this case, while the generalized plane strain assumption provides satisfactory results, the plane stress assumption gives inaccurate predictions.

None of the approaches, as referred to above, has ever been employed in the numerical analysis of a real masonry structure, which is mainly due to their limitation within the inelastic range. Subsequently, many researchers, including Andreaus (1996), Zhuge et al. (1998), Lourenco et al. (1998), Raffard et al. (2001), and Ushaksaraei and Pietruszczak (2002), conducted studies to develop a macroscopic failure criterion that can be incorporated to describe the mechanical behaviour of brick masonry. Andreaus (1996) employed the well-known failure criteria of Mohr-Coulomb, Saint-Venant, and Navier, to determine the failure stress state in masonry panels under in-plane loading. In this study, each criterion corresponded to different collapse mode such as slipping of mortar joints, cracking of bricks and middle plane spalling. The Coulomb frictional law, which has been modified to take into account the nonlinear dependence of shear strength on normal stress at high compression levels, captures slipping of mortar joints. Splitting can be predicted using the maximum tensile strain criterion (i.e. Saint-Venant criterion). Finally, the Navier criterion was associated with the middle plane spalling. These criteria were incorporated in the finite element analysis of a shear wall with openings under in-plane horizontal and vertical loads in two dimensions. Similarly, Lourenço et al. (1998) proposed a continuum model including two yield criteria for damage in tension and compression regimes. This approach consisted of an extension of conventional formulations for isotropic quasi-brittle materials employing different inelastic criteria for tension and compression. Rankine criterion for tension and Hill's criterion for compression were used in this study; however, the influence of the out-of-plane direction was not considered.

Raffard et al. (2001) also developed a numerical homogenization approach to identify the material properties for a homogenized stone masonry. In this approach, a modified Drucker-Prager yield criterion was incorporated to derive a macroscopic failure criterion in terms of a generalized deviatoric stress for the anisotropic materials. In addition, the identification of the material

properties was performed through a curve-fitting of the results obtained in the triaxial tests on stone masonry for different orientations of bed joints. Nonetheless, this model was not capable of assessing the failure condition in a real masonry structure due to its limitations in tension regime.

The most notable study in this context was performed by Ushaksaraei and Pietruszczak (2002). In that study, an anisotropic failure criterion for brick masonry was formulated within the framework of the Critical Plane Approach developed by Pietruszczak and Mroz (2001). The Critical Plane Approach is based on the notion of the existence of a critical plane, where the failure function reaches the maximum. Also, an extension of the critical plane framework was developed for the case of a nonlinear failure function which is more suitable for the class of brittle materials such as masonry. Subsequently, a macroscopic failure criterion in the quadratic form was proposed by incorporating a bilinear approximation for the structural masonry. Finally, the proposed failure criterion was incorporated in the 3D seismic analysis of the masonry walls of a power generation substation building located in Quebec.

1.3. Structure of the thesis

The main objective of this research is to implement a macroscopic failure criterion which describes the failure conditions in structural masonry. This thesis consists of four chapters. The next chapter introduces two frameworks which can be employed to formulate a macroscopic failure criterion for anisotropic materials (after Pietruszczak and Mroz, 2001). Then, a failure criterion incorporating both these frameworks, with a main focus on the microstructure tensor approach, is examined in the context of structural masonry. Subsequently, the identification procedure of the material parameters/functions incorporated in the failure criterion is discussed. At the end of this chapter, a numerical study including simulations of the experimental tests conducted by Page

(1981&1983) on the brick masonry is conducted to examine the performance of the framework. Chapter three is devoted to the application of this failure criterion in the finite element simulations of the shaking table test of a scaled four-storey masonry building as conducted at the Institute of Earthquake Engineering and Engineering Seismology (IEEES), Skopje. The numerical analysis is performed in the elastic range and the plastic admissibility of the predicted stress field is assessed by incorporating the proposed macroscopic failure criterion. The thesis ends with conclusions and recommendations for future works.

CHAPTER 2

MACROSCOPIC FAILURE CRITERION FOR STRUCTURAL MASONRY

2.1. Introduction

Duveau et al. (1998) conducted a comprehensive literature review on the formulation of failure criteria for anisotropic materials. On the basis of their study there are three main groups of criteria including continuous models, empirical continuous models, and discontinuous weakness planes-based models.

In the first category, the strength anisotropy is described through a mathematical approach that assumes a continuous variation of strength parameters. Hill (1948) derived the first failure criteria in this category for frictionless materials by extending von Mises isotropic theory. This approach was pursued by Tsai and Wu (1971) who introduced a failure criterion employing the first- and second-order terms in the stress components. The Hill criterion was also modified by Pariseau (1968) for rocks and soils in order to take into account the sensitivity of the mechanical behavior to the mean stress. Later, a more accurate and general formulation was derived in terms

of the invariants of stress and microstructure tensors (Boehler and Sawczuk, 1970). This failure criterion was subsequently simplified by Cowin (1986) using different orders of stress components and fabric tensors.

The failure criteria in the second category employ some empirical relations for the material parameters which are involved in an isotropic criterion. For instance, Jaeger (1960) employed the Mohr-Coulomb theory coupled with an empirical rule for variation of the cohesion coefficient while the internal friction remained constant. Then, in a similar way, a variation law for the friction coefficient was proposed by McLamore and Gray (1967) to improve Jaeger's criterion. The model's parameters could be identified by fitting the Mohr-Coulomb criterion to the experimental results of an extensive series of triaxial tests for different sample orientations.

The third category involves failure criteria in which the anisotropic material is considered as an isotropic body with sets of pre-defined weakness planes. Therefore, the failure can occur either within the matrix or along the weakness planes for different loading orientations. The first attempt in formulating such criterion was that by Jaeger (1960) who employed the Mohr-Coulomb function for both failure scenarios. A more accurate representation of this criterion was presented by Hoek (1964). The main improvement compared to Jaeger's model was proposing a non-linear failure envelope instead of the classic Mohr-Coulomb theory. It should be mentioned that implementation of this kind of failure criteria in a real problem requires identification of a large number of independent material parameters in addition to the information on orientation of the pre-existing weakness planes.

An alternative pragmatic approach to those discussed above is the formulation proposed by Pietruszczak and Mroz (2001). In this work, two conceptually different methodologies have been developed for specifying the failure conditions in anisotropic materials. The first one is the critical

plane approach in which the orientation of the potential failure plane is specified by solving a constrained optimazation problem for the maximum value of the failure function. The second approach incorporates a scalar anisotropy parameter η, which is expressed in terms of mixed invariants of stress and microstructure tensors. These two frameworks are reviewed in this chapter and later employed to describe the conditions at failure for structural masonry.

2.2. Formulation of Macroscopic Failure Criterion for Structural Masonry

The failure criterion for the structural masonry considered here has the same functional form as that employed for sedimentary rocks by Pietruszczak and Haghighat (2015). It incorporates both approaches mentioned above, i.e. critical plane framework and microstructure tensor approach. The general form of the failure function is defined as follows:

$$F = max(F_1, F_2) \tag{2.1}$$

$F_1 = F(\sigma_{ij}, a_{ij})$ Failure function incorporating microstructure tensor

$F_2 = f(\tau, \sigma) - c(n_i)$ Failure function based on Critical Plane Approach

For an arbitrary stress state, the values of these two failure functions are calculated, and the maximum value of F is established. In the compression regime, the failure is governed by the failure function incorporating the microstructure tensor approach, while in the tension regime the failure function based on the Critical Plane framework is active. In the following sections, these failure functions will be explained in detail.

2.2.1. Microstructure Tensor Approach

This approach employs a scalar anisotropy parameter which is a function of mixed invariants of stress and microstructure tensors (Pietruszczak and Mroz, 2001). A microstructure tensor a_{ij} is introduced as a measure of material fabric, e.g. the arrangement of intergranular contacts, the crack or voids patterns, the pore size distribution, etc. The eigenvectors of the microstructure tensors, $e_i^{(\alpha)}$, α =1,2,3, represent the principal material axes. The microstructure tensor a_{ij} may be defined as follows:

$$a_{ij} = a_1 e_i^{(1)} e_j^{(1)} + a_2 e_i^{(2)} e_j^{(2)} + a_3 e_i^{(3)} e_j^{(3)} = a_1 m_{ij}^{(1)} + a_2 m_{ij}^{(2)} + a_3 m_{ij}^{(3)} \qquad (2.2)$$

where, $m_{ij}^{(\alpha)} = e_i^{(\alpha)} e_j^{(\alpha)}$ are the structure-orientation tensors and a_1, a_2, a_3 are the principal values of the microstructure tensor.

In the most general representation, the failure criterion is expressed as a function of both the stress state σ_{ij} and microstructure tensor a_{ij}, i.e.

$$F_1 = F(\sigma_{ij}, a_{ij}) = F\ (T_{ij}T_{pq}\sigma_{pq}, T_{ip}T_{jq}a_{pq}) \qquad (2.3)$$

$$= F(tr\boldsymbol{\sigma}, tr\boldsymbol{\sigma}^2, tr\boldsymbol{\sigma}^3, tr\boldsymbol{a}, tr\boldsymbol{a}^2, tr\boldsymbol{a}^3, tr(\boldsymbol{\sigma a}), tr(\boldsymbol{\sigma}^2\boldsymbol{a}), tr(\boldsymbol{\sigma a}^2), tr(\boldsymbol{\sigma}^2\boldsymbol{a}^2)) = 0$$

Here, T_{ij} is the transformation tensor. The above representation is too complex to be used for practical applications. Thus, a simplified formulation has been developed (Pietruszczak and Mroz, 2001) , whereby the anisotropy measures are defined in terms of relative orientation of principal axes of stress and microstructure tensors. These descriptors are then related to the strength parameters which are assumed to be orientation dependent.

This formulation uses the concept of 'generalized loading vector' to characterize the loading direction with respect to the principal axes of the material. It is defined as:

$$L_i = L_j e_k^{(i)};\ L_j = (\sigma_{j1}{}^2 + \sigma_{j2}{}^2 + \sigma_{j3}{}^2)^{1/2};\ (i, j=1, 2, 3) \tag{2.4}$$

or

$$L_1 = (\sigma_{11}{}^2 + \sigma_{12}{}^2 + \sigma_{13}{}^2)^{1/2};\ L_2 = (\sigma_{12}{}^2 + \sigma_{22}{}^2 + \sigma_{23}{}^2)^{1/2}; \tag{2.5}$$

$$L_3 = (\sigma_{13}{}^2 + \sigma_{23}{}^2 + \sigma_{33}{}^2)^{1/2}$$

As can be seen from the above equations, the components of L_i are the magnitudes of traction vectors on the planes normal to the principal material axes. Also,

$$L_i{}^2 = e_k^{(i)}\sigma_{kj}e_l^{(i)}\sigma_{lj} = tr\left(m_{kp}^{(i)}\sigma_{ql}\sigma_{lk}\right);\quad L_kL_k = \sigma_{kj}\sigma_{kj} = tr\left(\sigma_{kl}\sigma_{lj}\right) \tag{2.6}$$

The generalized loading vector is a unit vector along L_i, so that

$$l_i = \frac{L_i}{(L_kL_k)^{1/2}} = \left[\frac{e_k^{(i)}\sigma_{kj}e_m^{(i)}\sigma_{mj}}{\sigma_{pq}\sigma_{pq}}\right]^{\frac{1}{2}} \tag{2.7}$$

A scalar anisotropy parameter used in this approach is defined as the projection of the microstructure tensor a_{ij} on the loading direction l_i :

$$\eta = a_{ij}l_il_j = \left[\frac{a_{ik}\sigma_{ij}\sigma_{kj}}{\sigma_{pq}\sigma_{pq}}\right] = a_1\frac{tr(m^{(1)}\sigma^2)}{tr\sigma^2} + a_2\frac{tr(m^{(2)}\sigma^2)}{tr\ ^2} + a_3\frac{tr(m^{(3)}\sigma^2)}{tr\ ^2} = \frac{tr(a\sigma^2)}{tr\ ^2} \tag{2.8}$$

Thus, this scalar variable η is the ratio of the joint invariant of the stress and the microstructure tensor to the second invariant of the stress tensor. It describes the effect of the loading orientation

with respect to the principal material axes. Note that this measure is independent of the stress magnitude. The representation (2.8) can be expressed as:

$$\eta = \eta_0(1 + A_{ij}l_i l_j) \tag{2.9}$$

Where, $A_{ij} = \text{dev}\,(a_{ij})/\eta_0$ is a symmetric traceless operator. The above equation can be generalized by considering higher order tensors.

$$\eta = \eta_0(1 + A_{ij}l_i l_j + A_{ijkl}l_i l_j l_k l_l + \cdots) \tag{2.10}$$

For simplicity, the higher order tensors can be defined as dyadic products of second-order tensors, instance. $A_{ijkl} = b_1 A_{ij}A_{kl}$ and $A_{ijklmn} = b_2 A_{ij}A_{kl}A_{mn}$. Therefore, the representation of anisotropy parameter η becomes

$$\eta = \eta_0(1 + A_{ij}l_i l_j + b_1(A_{ij}l_i l_j)^2 + b_2(A_{ij}l_i l_j)^3 + b_3(A_{ij}l_i l_j)^4 + \cdots) \tag{2.11}$$

Here, b's are constants.

With regards to the above-stated simplification, the failure function (2.3) can be represented in the following simplified form:

$$F = F(\sigma_{ij}, a_{ij}) = F(tr\boldsymbol{\sigma}, tr\boldsymbol{\sigma}^2, tr\boldsymbol{\sigma}^3, \eta) \tag{2.12}$$

Also, the failure function (2.12) may be expressed in the form:

$$F = F(\sigma_{ij}, a_{ij}) = F(I_1, J_2, J_3, \eta) \tag{2.13}$$

where, I_1 is the first stress invariant, and J_2, J_3 are the basic invariants of the stress deviator. Considering that the anisotropy parameter η is orientation dependent, the above failure function can be employed for anisotropic materials by assuming that the strength parameters have a similar

representation to that of Equation (2.11). The number of strength parameters depends on the failure criterion used and the type of the material.

Here, Mohr-Coulomb criterion is adopted to define the conditions at failure

$$F = \sqrt{3}\bar{\sigma} - \eta_f g(\theta)(\sigma_m + C) \tag{2.14}$$

where

$$g(\theta) = \frac{3-\sin}{2\sqrt{3}\cos\theta - 2\sin\theta\sin}; \quad \eta_f = \frac{2\sqrt{3}\sin\phi}{3-\sin\phi}; \quad C = c\cot\emptyset \tag{2.15}$$

In this expression, $\emptyset$, c are the angle of friction and cohesion, respectively, and θ denotes Lode's angle. The stress invariants σ_m ,$\bar{\sigma}$, and θ are function of the basic stress invariants, i.e.

$$\bar{\sigma} = (J_2)^{1/2}; \ \ \sigma_m = -\frac{1}{3} I_1; \theta = \frac{1}{3}\sin^{-1}\left(\frac{-3\sqrt{3}}{2}\frac{J_3}{\bar{\sigma}^3}\right) \tag{2.16}$$

The extension of the above failure criterion to anisotropic material may be obtained by expressing the orientation-dependent strength parameters, in this case η_f and C, in a form analogous to Equation (2.11). However, the parameter C associated with the strength under hydrostatic tension is a material constant, i.e., it is orientation independent. This is because under hydrostatic tension the loading vector components are equal to

$$l_1 = l_2 = l_3 = 1/\sqrt{3} \tag{2.17}$$

Since, in the principal material system, $A_{ij} = 0$ for $i \neq j$ and also $A_{ii} = 0$, it can be concluded that

$$A_{ij}l_i l_j = \ (A_1 + A_2 + A_3)/3 \equiv 0 \tag{2.18}$$

which implies that $C = const$. Therefore, the only orientation-dependent strength parameter in this case is η_f which can be defined as

$$\eta_f = \widehat{\eta_f}(1 + A_{ij}l_il_j + b_1(A_{ij}l_il_j)^2 + b_2(A_{ij}l_il_j)^3 + b_3(A_{ij}l_il_j)^4 + \cdots) \quad (2.19)$$

To identify the material constants embedded in the Equation (2.19), the information of the failure conditions in samples tested at different orientations of the bedding plane β should be obtained, which will be discussed in detail further.

2.2.2. Critical Plane Framework

In the critical plane framework, the orientation of the failure plane is specified through the optimization of the failure function with respect to the orientation. The failure function is defined in terms of normal and shear stress components σ, τ, acting on the plane with unit normal n_i , as well as the strength parameter c (Ushaksaraei and Pietruszczak, 2002)

$$F_2 = f(\tau, \sigma) - c(n_i) \quad (2.20)$$

Here,

$$\sigma = \sigma_{ij}n_in_j \quad (2.21)$$

$$\tau = \sigma_{ij}n_is_j \quad (2.22)$$

where s_i is an arbitrary unit vector normal to n_i

$$n_is_i = 0 \quad (2.23)$$

Since the strength parameter c is orientation-dependent here, the function $c(n_i)$ may have a representation similar to Equation (2.11), i.e.:

$$c(n_i) = c_0(1 + \Omega_{ij} n_i n_j + b_1(\Omega_{ij} n_i n_j)^2 + b_2(\Omega_{ij} n_i n_j)^3 + b_3(\Omega_{ij} n_i n_j)^4 + \cdots) \quad (2.24)$$

The eigenvectors of Ω_{ij} define the principal material axes. For an orthotropic material, there are two independent eigenvalues of Ω_{ij} (since Ω_{ii}= 0), and the number of eigenvalues is reduced to one for a transversely isotropic materials.

The onset of failure and the orientation of the critical plane can be specified by solving the following constrained optimization problem

$$max_{n_i} F = max_{n_i}(f(\sigma, \tau) - c(n_i)) = 0 \; ; \; n_i n_i = 1 \quad (2.25)$$

The method of Lagrange multipliers or other suitable optimization methods can be incorporated to solve the above equations. Depending on the type of material, different failure criteria can be utilized to describe the behavior.

In this framework, tension cut-off criterion is employed to measure the tension resistance of masonry panel. The notion of tension cut-off criterion suggests that the tensile failure occurs when the normal component of traction vector t_i acting on the localization plane reaches the value of the strength parameter c. In this case, the failure criterion (2.25) becomes:

$$max_{n_i} F = max_{n_i}(\sigma - c(n_i)) = 0 \quad (2.26)$$

The identification of the material constants ($c_0, \Omega_1, b_1, b_2,$ and etc.) embedded in the general distribution of $c(n_i)$, Equation (2.24), requires high-order polynomial fitting to it, which will be explained further in the next section.

2.3. Identification Procedure of Material Parameters/Functions in the Failure Criterion

2.3.1. Microstructure Tensor Approach

This section explains the identification procedure of the constants embedded in the spatial distribution of the strength parameters in the failure function. The first step of this procedure is to estimate the value of the material parameter C appearing in the failure condition. For this purpose, it is convenient to express the Mohr-Coulomb failure function in terms of principal stresses, i.e.

$$\frac{1}{2}(\sigma_I - \sigma_{III}) - \frac{1}{2}(\sigma_I + \sigma_{III})\sin\phi - C\sin\phi = 0 \tag{2.27}$$

Note that, in this thesis, σ_1 and σ_2 refer to the horizontal and vertical stress, respectively. This notation is consistent with that used by Page's in presenting the results of his experimental tests. At the same time, the principal stresses appearing in Mohr-Coulomb criterion have been defined by Roman numerals.

For the tests involving uniaxial compression and biaxial compression-tension, the minimum principal stress (σ_{III}) is zero, while the vertical stress is the maximum principal stress (σ_I). Therefore, based on the results of these test, the value of C can be estimated by plotting the linear Mohr-Coulomb envelopes in $\frac{1}{2}(\sigma_I - \sigma_{III})$ vs $\frac{1}{2}(\sigma_I + \sigma_{III})$ space.

The identification process is based here on the results of experimental tests conducted by Page (1983) that involved both biaxial compression-tension and uniaxial compression at different orientations of sample (ranging from 0 to 90 degrees). The main results, in terms of averages for

all tests reported by Page, are shown in Table 2.1. In this table, β represents the orientation of bed joints, f_c is the uniaxial compression strength, and α is the ratio of horizontal tensile stress to vertical compressive stress at failure.

β	$f_c(MPa)$	$\alpha = 0.2$		$\alpha = 0.1$	
		Compression stress (σ_2) (MPa)	Tension stress (σ_1) (MPa)	Compression stress (σ_2) (MPa)	Tension stress (σ_1) (MPa)
0	7.670	2.792	0.558	3.795	0.348
22.5	5.663	2.343	0.455	3.462	0.325
45	4.804	1.915	0.377	2.589	0.235
67.5	2.866	1.489	0.295	1.596	0.146
90	4.371	0.958	0.194	2.305	0.190

Table 2.1. Results of Experimental Uniaxial Compression and Biaxial Compression Tension Tests, Page(1983)

The value of the parameter C is assessed for each angle by best-fitting the experimental data with a linear Mohr-Coulomb approximation, Figure 2.1.

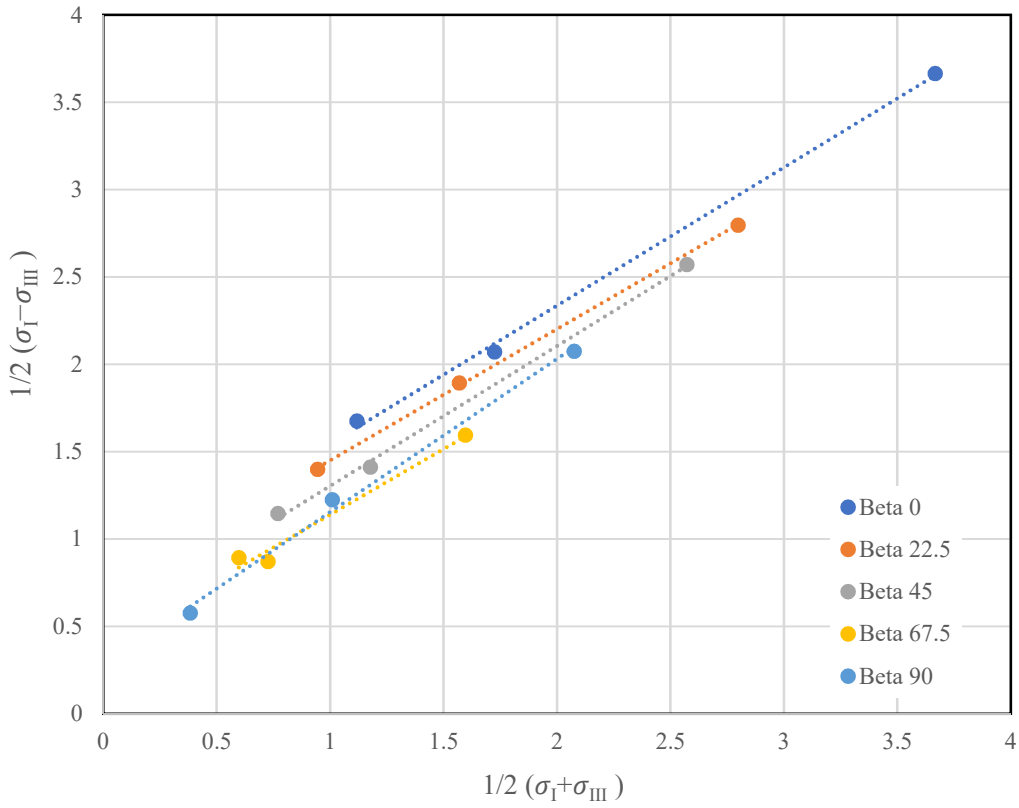

Figure 2.1 Linear Approximation (Mohr-Coulomb) of Failure Condition for Different Orientation of Bed Joints

The final estimate of C is obtained by taking the maximum value over the set of orientations considered. This results in $C = 0.956$, which has been used in further analysis. It is important to note that this parameter has no physical meaning as the strength under hydrostatic tension is governed by the cut off criterion (2.20), in which $c(n_i) < C$.

β	C (MPa)
0	0.956
22.5	0.930
45	0.628
67.5	0.518
90	0.319
Max	0.956

Table 2.2. Parameter (C) for different bed joint orientations

After the determination of the value of C, the next step is to identify the coefficients $(\widehat{\eta_f}, A_1, b_1, b_2, b_3)$ appearing in the distribution function of the strength parameter η_f, i.e. Equation (2.19). Note that η_f can be expressed as a function of the friction angle through the relation

$$\eta_f = \frac{6\sin\phi}{3-\sin\phi} \tag{2.28}$$

The value of ϕ can be calculated from the Mohr-Coulomb failure function (2.27) by imposing the conditions of uniaxial compression, i.e.

$$\sigma_I = f_c; \sigma_{III} = 0$$

$$\frac{1}{2}f_c - \frac{1}{2}f_c\sin\phi - C\sin\phi = 0$$

$$\sin\phi = \frac{f_c}{f_c+2C} \tag{2.29}$$

Table 2.3 shows the obtained values of ϕ as well as the corresponding values of the parameter η_f. The results correspond to all uniaxial compression tests conducted by Page (1983) at the different orientations of bed joints.

β	$f_c(MPa)$	$C(MPa)$	ϕ	l_2	$1-3{l_2}^2$	η_f
0	7.993	0.956	0.939	1.000	-2.000	2.208
0	8.231	0.956	0.947	1.000	-2.000	2.225
0	7.109	0.956	0.908	1.000	-2.000	2.138
0	7.347	0.956	0.917	1.000	-2.000	2.158
22.5	4.890	0.956	0.802	0.924	-1.561	1.891
22.5	5.366	0.956	0.829	0.924	-1.561	1.955
22.5	5.638	0.956	0.843	0.924	-1.561	1.988
22.5	6.760	0.956	0.894	0.924	-1.561	2.106
45	6.208	0.956	0.870	0.707	-0.500	2.052
45	4.099	0.956	0.750	0.707	-0.500	1.765
45	4.541	0.956	0.781	0.707	-0.500	1.839
45	5.119	0.956	0.815	0.707	-0.500	1.923
45	5.459	0.956	0.834	0.707	-0.500	1.967
67.5	3.376	0.956	0.692	0.383	0.561	1.622
67.5	2.321	0.956	0.580	0.383	0.561	1.342
67.5	2.560	0.956	0.609	0.383	0.561	1.415
67.5	3.206	0.956	0.677	0.383	0.561	1.583
90	3.640	0.956	0.715	0.000	1.000	1.678
90	4.218	0.956	0.759	0.000	1.000	1.786
90	4.626	0.956	0.786	0.000	1.000	1.852
90	5.000	0.956	0.809	0.000	1.000	1.906

Table 2.3. Values of η_f for different bedding plane orientations

It should be noted that a more general identification procedure would involve a case of triaxial compression with confining pressure, P_0. In order to illustrate it, consider the sample geometry as shown in Figure 2.2.

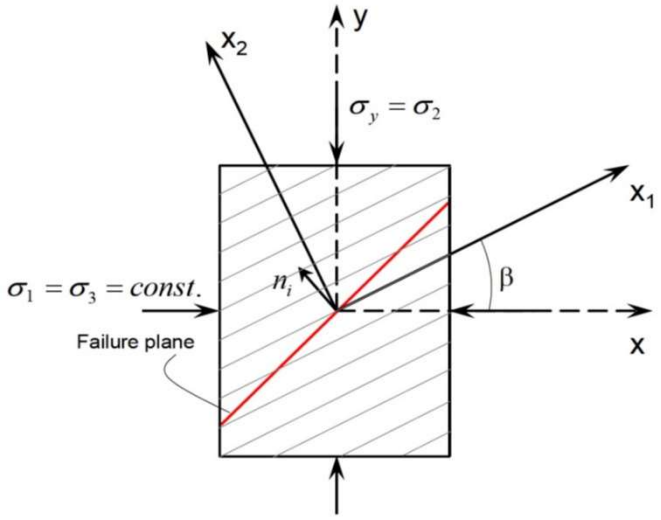

Figure 2.2 Geometry of the Sample in Uniaxial Compression Test (Pietruszczak, 2010)

For this problem, the stress tensor will have the following form in the local coordinate system

$$\sigma_{ij} = \begin{bmatrix} cos^2(\beta)P_0 + sin^2(\beta)\sigma_2 & -\cos(\beta)\sin(\beta)P_0 + \cos(\beta)\sin(\beta)\sigma_2 & 0 \\ -\cos(\beta)\sin(\beta)P_0 + \cos(\beta)\sin(\beta)\sigma_2 & sin^2(\beta)P_0 + cos^2(\beta)\sigma_2 & 0 \\ 0 & 0 & P_0 \end{bmatrix} \tag{2.30}$$

In this way, the components of loading vector, Equation (2.4), become

$$L_1{}^2 = \sigma_{11}{}^2 + \sigma_{12}{}^2 + \sigma_{13}{}^2 = cos^2(\beta)P_0{}^2 + sin^2(\beta)\sigma_2{}^2$$

$$L_2{}^2 = \sigma_{21}{}^2 + \sigma_{22}{}^2 + \sigma_{23}{}^2 = sin^2(\beta)P_0{}^2 + cos^2(\beta)\sigma_2{}^2$$

$$L_3{}^2 = \sigma_{31}{}^2 + \sigma_{32}{}^2 + \sigma_{33}{}^2 = P_0{}^2 \tag{2.31}$$

Also the unit vector, l_i, takes the following form

$$l_1^2 = \frac{L_1^2}{L_1^2 + L_2^2 + L_3^2} = \frac{cos^2(\beta)P_0{}^2 + sin^2(\beta)\sigma_2{}^2}{2P_0{}^2 + \sigma_2{}^2}$$

$$l_2^2 = \frac{L_2^2}{L_1^2 + L_2^2 + L_3^2} = \frac{sin^2(\beta){P_0}^2 + cos^2(\beta){\sigma_2}^2}{2{P_0}^2 + {\sigma_2}^2}$$

$$l_3^2 = \frac{L_3^2}{L_1^2+L_2^2+L_3^2} = \frac{{P_0}^2}{2{P_0}^2+{\sigma_2}^2} \tag{2.32}$$

For a transversely isotropic material, there is one eigenvalue for the fabric tensor A_{ij}. Also, the fabric tensor, A_{ij} is a traceless tensor,i.e., $A_{ii} = 0$. Thus, $A_1 = A_3$ and $A_2 = -2A_1$. In addition, $l_1^2 + l_2^2 + l_3^2 = 1$. Thus

$$A_{ij}l_il_j = A_1l_1^2 + A_2l_2^2 + A_3l_3^2 = A_1l_1^2 - 2A_1l_2^2 + A_1l_3^2 = A_1(1 - 3l_2^2) \tag{2.33}$$

Therefore, the representation of η_f , Equation (2.19), becomes

$$\eta_f = \widehat{\eta_f}(1 + A_1\xi + b_1{A_1}^2\xi^2 + b_2{A_1}^3\xi^3 + b_3{A_1}^4\xi^4 \dots) \tag{2.34}$$

in which

$$\xi = (1 - 3l_2^2) \tag{2.35}$$

When the confining pressure (P_0) is zero, l_2 equals $\cos\beta$. Thus, Equation (2.35) for this case is reduced to

$$\eta_f = \widehat{\eta_f}(1 + A_1(1 - 3cos^2(\beta)) + b_1{A_1}^2\left(1 - 3cos^2(\beta)\right)^2 + \cdots) \tag{2.36}$$

Figure 2.3 depicts the variation of η_f against ξ. A fourth-order approximation is fitted to the diagram to find the set of coefficients appearing in (2.35). The identified coefficients are provided in Table 2.4.

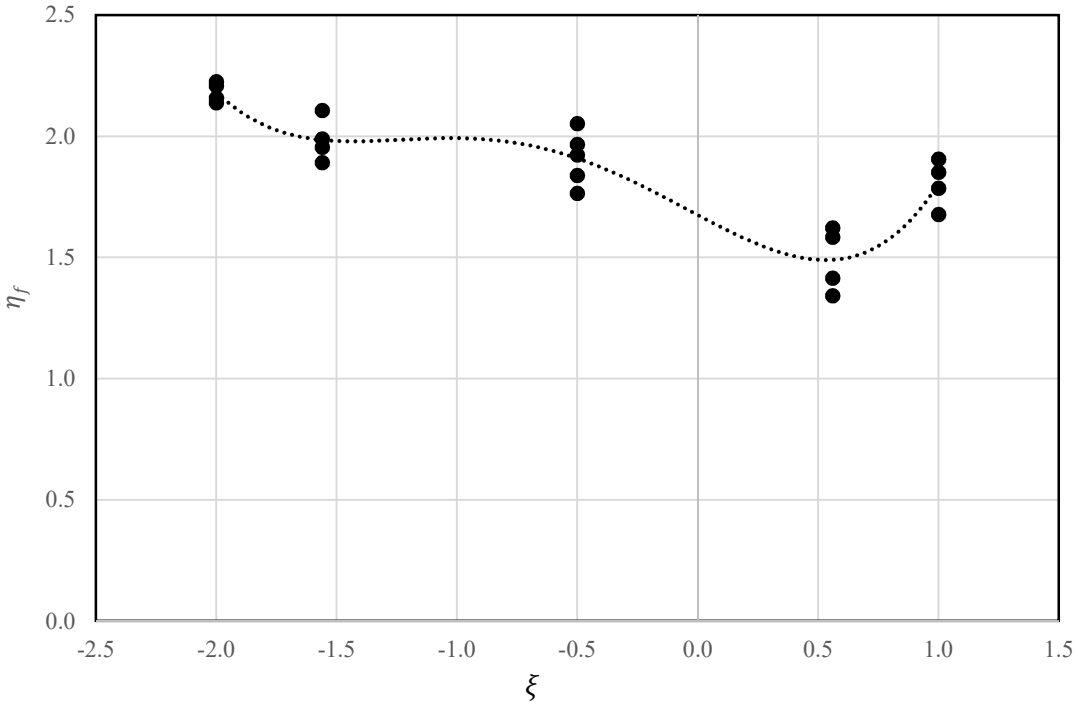

Figure 2.3 Distribution of η_f vs ξ

η_f	1.676
A_1	-0.314
b_1	0.330
b_2	-8.322
b_3	10.313

Table 2.4 Coefficients of function $\eta_f(l_i)$ for uniaxial compression test

2.3.2. Critical Plane Framework

Similar to microstructure tensor approach, the constants appearing in the spatial distribution of function $c(n_i)$, Eq (2.24), should be identified in this framework. These independent parameters c_0, b_1, b_2, b_3, and Ω_1 are specified based on the experimental data of uniaxial tension tests reported by Page (1983). Figure 2.4 shows the polar distribution of function $c(n_i)$ which has

been depicted by Ushaksaraei and Pietruszczak (2002) by assuming that the ratio of tensile strength on plane at 45° to the tensile strength along the bed joints lies between 3 and 4. The values of the parameter c are summarized in Table 2.5.

β	$1-3cos^2\beta$	c
0	-2.00	0.24
10	-1.91	0.318
20	-1.65	0.498
22.5	-1.56	0.552
30	-1.25	0.708
40	-0.76	0.873
45	-0.50	0.911
45	-0.50	0.911
50	-0.24	0.906
55	0.01	0.881
60	0.25	0.825
67.5	0.56	0.693
70	0.65	0.648
80	0.91	0.476
90	1.00	0.40

Table 2.5 Values of $c(n_i)$ for different orientations of sample

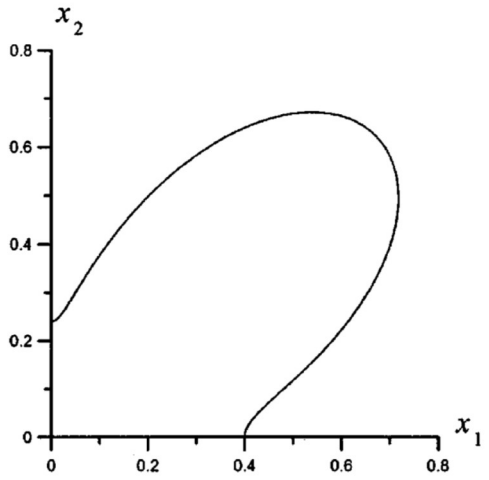

Figure 2.4 Polar distribution of $c(n_i)$ (Ushaksaraei.and Pietruszczak , 2002)

By fitting a fourth-order polynomial function to the distribution of function $c(n_i)$, Figure 2.5, the following set of coefficients is obtained as shown in Table 2.6.

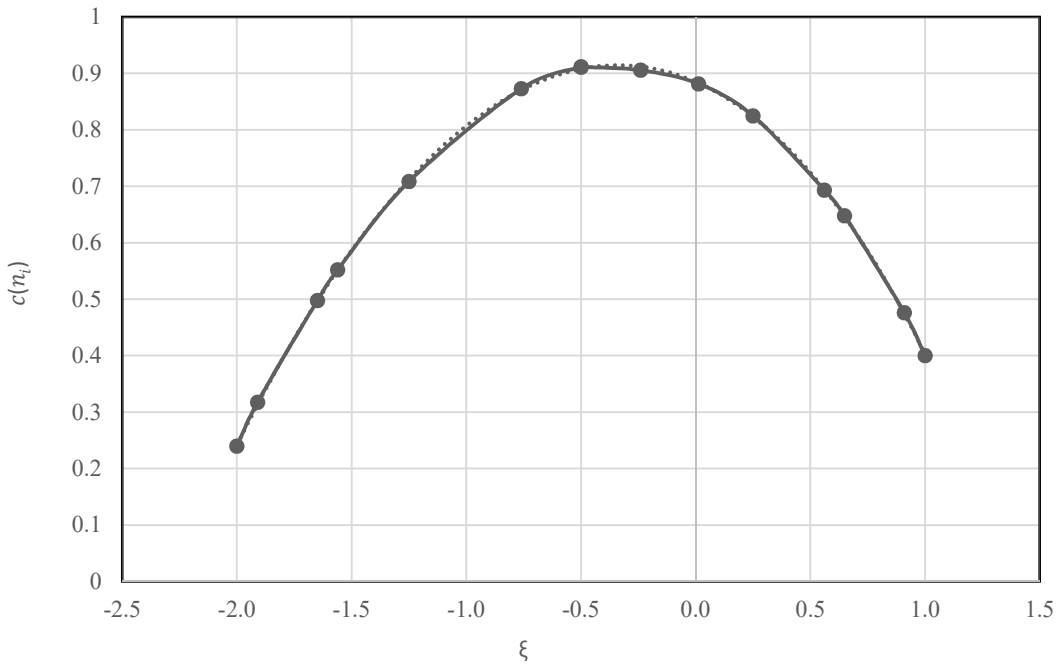

Figure 2.5 Variation of $c(n_i)$ vs ξ

.

c_0	0.885
Ω_1	-0.200
b_1	-7.707
b_2	3.523
b_3	-4.482

Table 2.6 Coefficients corresponding to distribution function of $c(n_i)$

2.4. Model Verification against Experimental Data

Several numerical simulations were conducted using the material parameters identified in the previous section to evaluate the performance of the proposed failure criterion. In this study, the numerical results are compared with those of experimental tests performed by Page (1981, 1983),

which included uniaxial compression, uniaxial tension, biaxial compression-compression, and biaxial compression-tension at different orientations of bed joint.

First, the mechanical response of the sample under uniaxial compression loading is studied. Figure 2.6 shows the variation of axial compressive strength as a function of the orientation of bedding planes. For low values of β (from 0^o to 40^o), the failure involves the formation of macrocracks in the direction close to the head joints. The failure mode changes at $\beta \approx 40^o$ as the damage is localized in the bed joints. For the above failure mechanism, the compressive strength first decreases significantly and reaches its minimum value at $\beta \approx 67.5^o$, and then increases gradually. In general, the numerical results are quite consistent with the experimental data, provided by Page (1983), especially in terms of representing the transition in the failure mode.

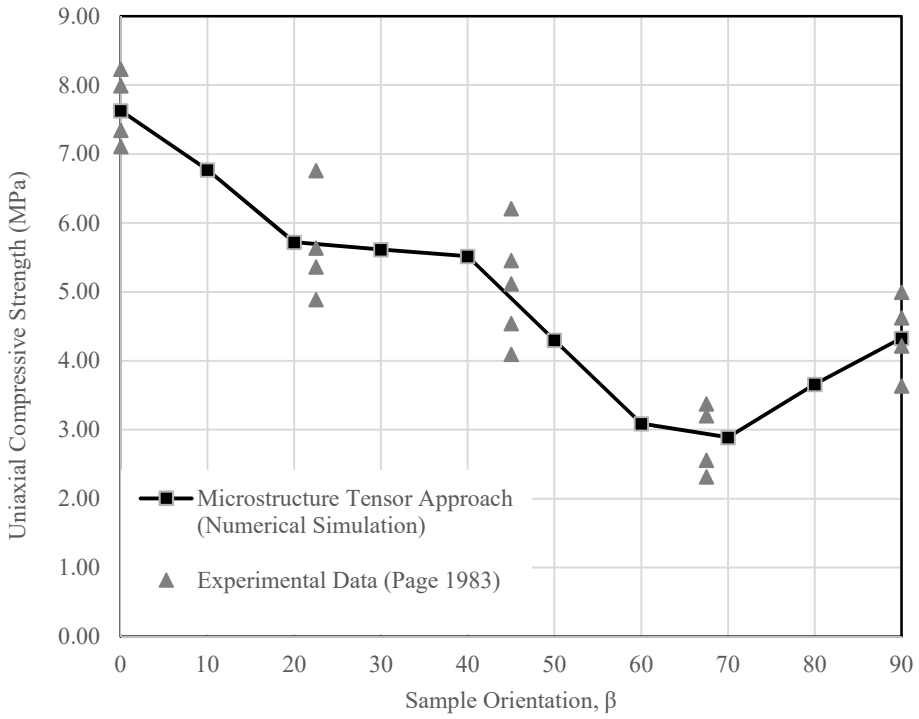

Figure 2.6 Comparison of Numerical Results with Experimental Data (Page1983), Uniaxial Compression Test

The variation of tensile strength and the critical plane orientation with the bed joints angle is

presented in Figures 2.7 (a) and (b), respectively. Figure 2.7 (b) indicates a transition in the failure plane orientation; i.e. the failure plane shifts from along the bed joints to the orientation perpendicular to it at $\beta = 45^o$. In addition, the tensile strength increases gradually until the bed joints angle reaches 45 degrees, then grows significantly at $\beta = 45^o$, and finally decreases gradually. It should be noted that the definition of the bed joints angle in this simulation is different from its definition in Page's uniaxial tension test. Here, β equals zero when the tension is perpendicular to the bed joints, and when the load is applied along the bed joints, $\beta = 90^o$. The predicted trend is generally consistent with the experimental results obtained by Page (1983).

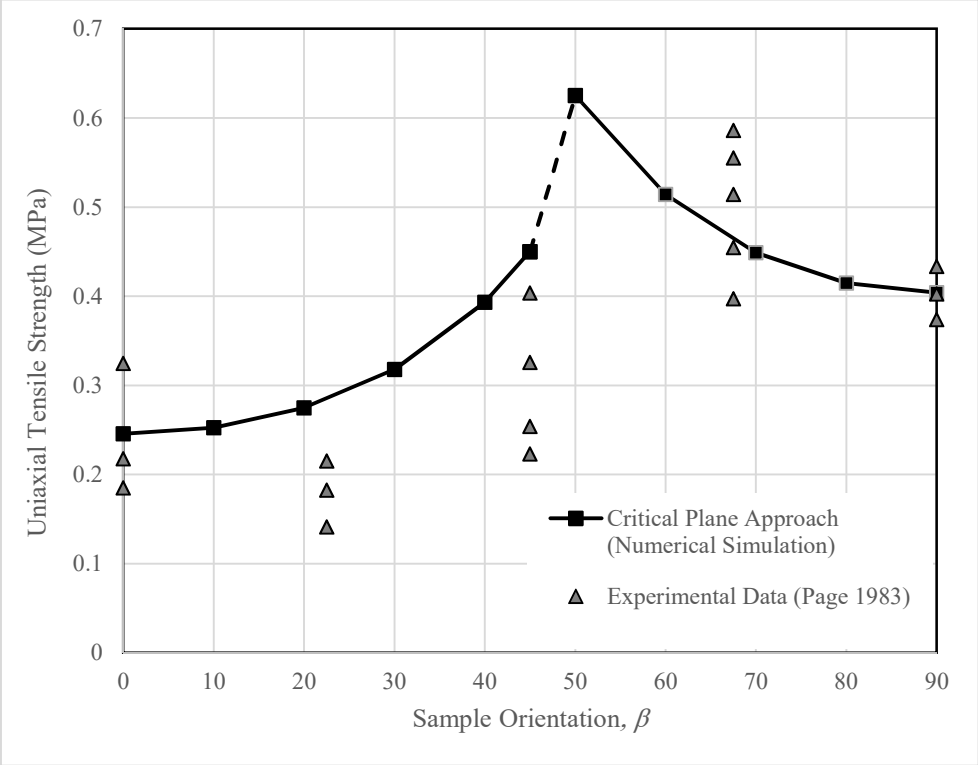

a)

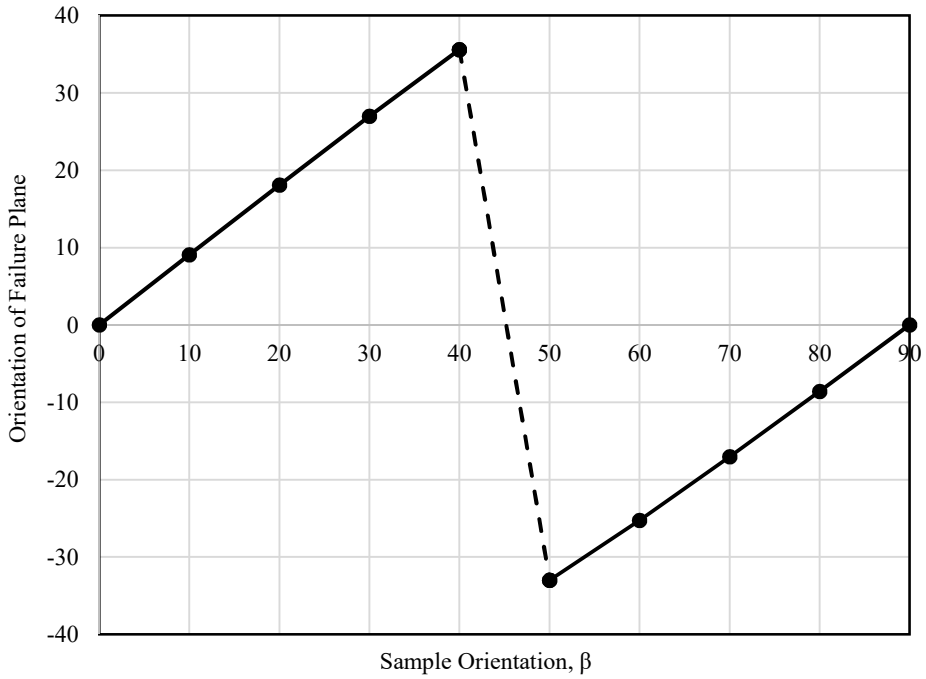

b)

Figure 2.7 Variation of a) Uniaxial Tensile Strength and b) Failure Plane Orientation vs. Orientation of Bed Joints, β

The next stage of the numerical study is the simulation of a set of inplane biaxial compression-tension tests performed by Page (1983) to evaluate the performance of the proposed macroscopic failure criterion. In these tests, the loading involves a constant ratio of compressive to tensile stress, including 0, -0.5, -0.25, -0.1, -0.033, and -∞. Figure 2.8 shows the predicted failure envelopes for different orientations of bed joints. The numerical results are fairly consistent with the experimental data, especially that the experimental scatter is quite significant.

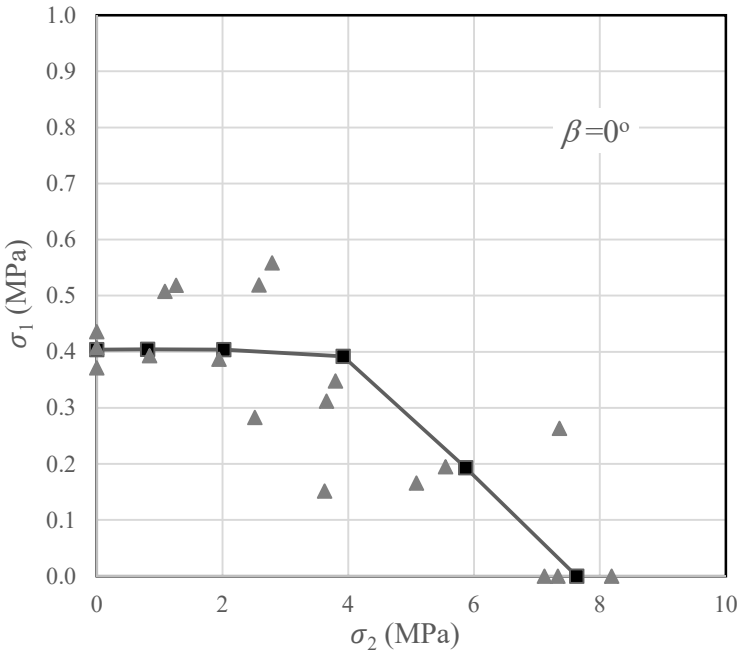
β=0°
σ1 (MPa)
σ2 (MPa)

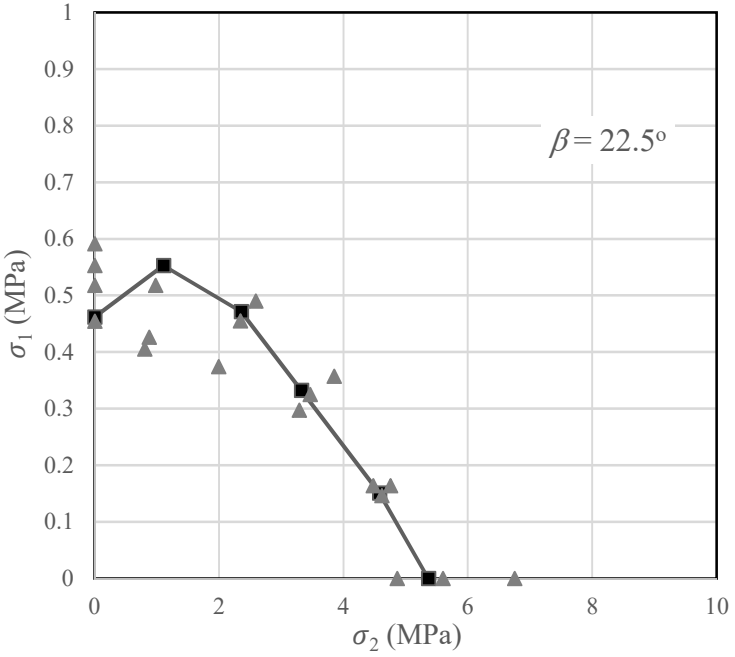
β= 22.5°
σ1 (MPa)
σ2 (MPa)

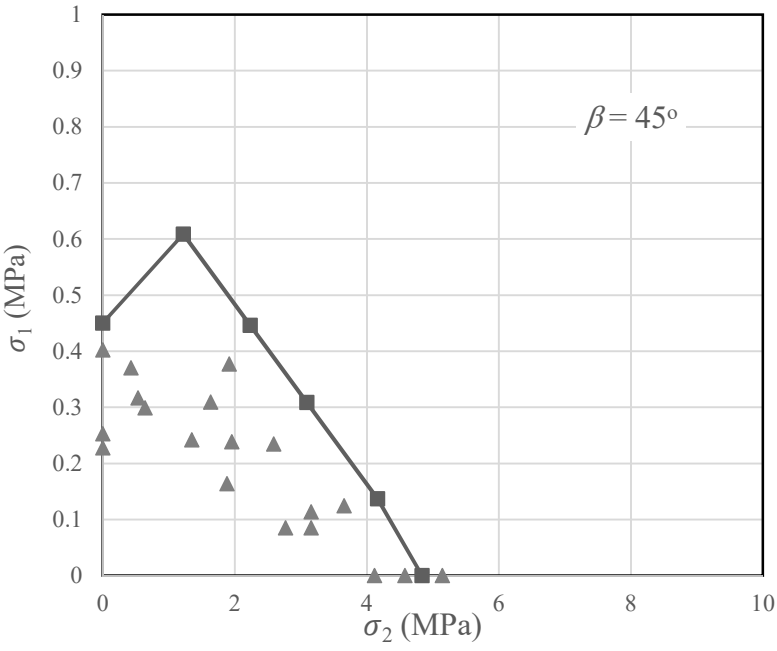
β= 45°
σ1 (MPa)
σ2 (MPa)

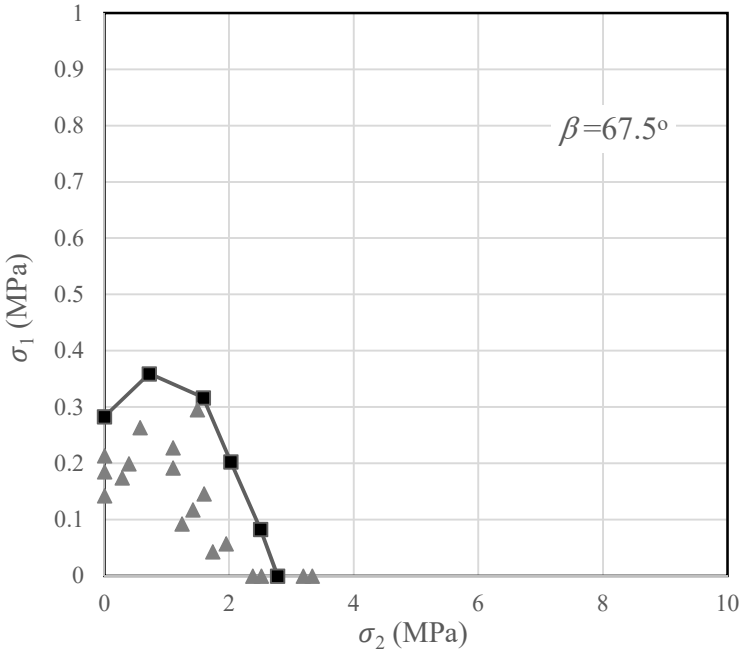
β=67.5°
σ1 (MPa)
σ2 (MPa)

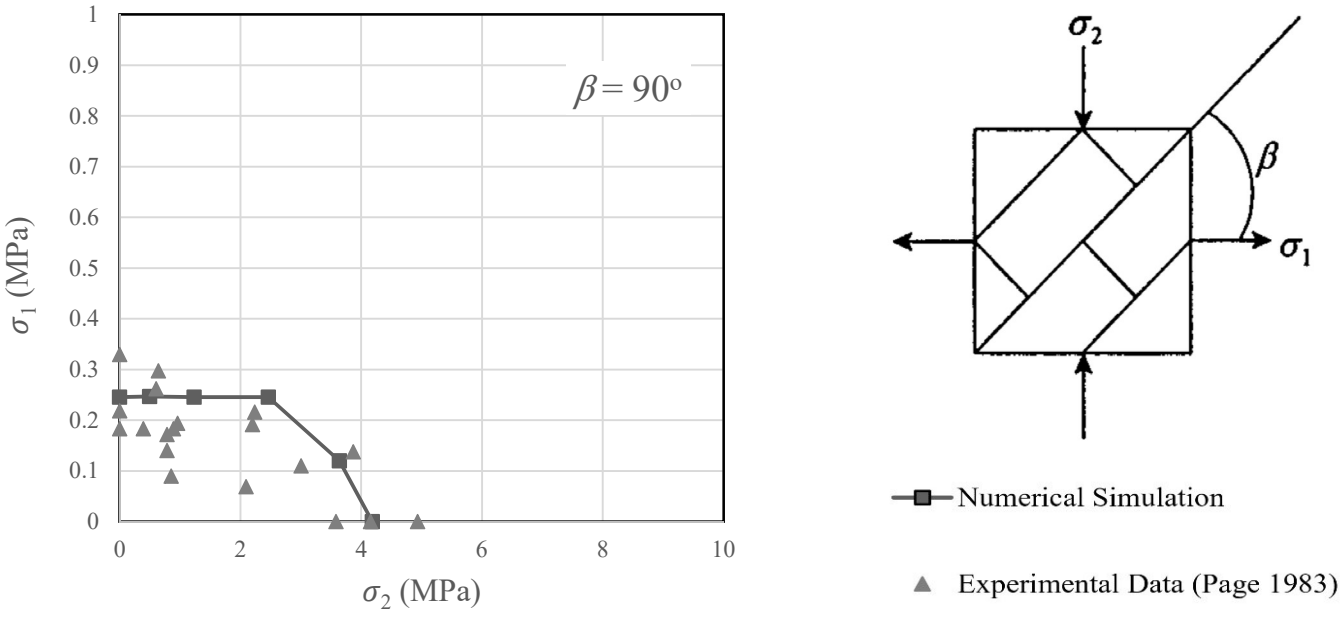

Figure 2.8 Predicted Failure Surfaces of In Plane Biaxial Compression-Tension Tests

Finally, the sets of predictions corresponding to the biaxial compression tests carried out by Page (1981) are represented in Figure 2.9. In these tests, the out–of-plane stress is zero, and as such it is the minor principal stress. Also, the loading path is similar to the biaxial compression-tension test, i.e., the stress ratio is constant. As discussed previously, the assumption of transverse isotropy is not valid here, and the out-of-plane characteristics have a profound influence on the behavior of structural masonry. For this reason, another set of simulations has been performed considering the orthotropic properties of the structural masonry. The results of these simulations are shown by a broken line in Figure 2.9. In this case the fabric tensor A_{ij} has two independent eigenvalues, A_1 and A_2, so that Equation (2.34) should be modified to

$$A_{ij}l_il_j = A_1{l_1}^2 + A_2{l_2}^2 - (A_1 + A_2)(1 - ({l_1}^2 + {l_2}^2)) \tag{2.37}$$

Thus, there are now six unknown coefficients $\widehat{\eta_f}$, b_1, b_2, b_3, A_1, and A_2, in the formulation of η_f, Eq. (2.19). In this case, the values of η_f can be calculated from Eqs. (2.28) and (2.29) again, however f_c should be replaced by the corresponding value of the vertical stress. By solving a nonlinear equations system, the following coefficients have been obtained:

$$\eta_f = 1.8579 \quad A_1 = 0.109 \quad A_2 = 0.345 \quad b_1 = 0.157 \quad b_2 = -6.114 \quad b_3 = 4.743$$

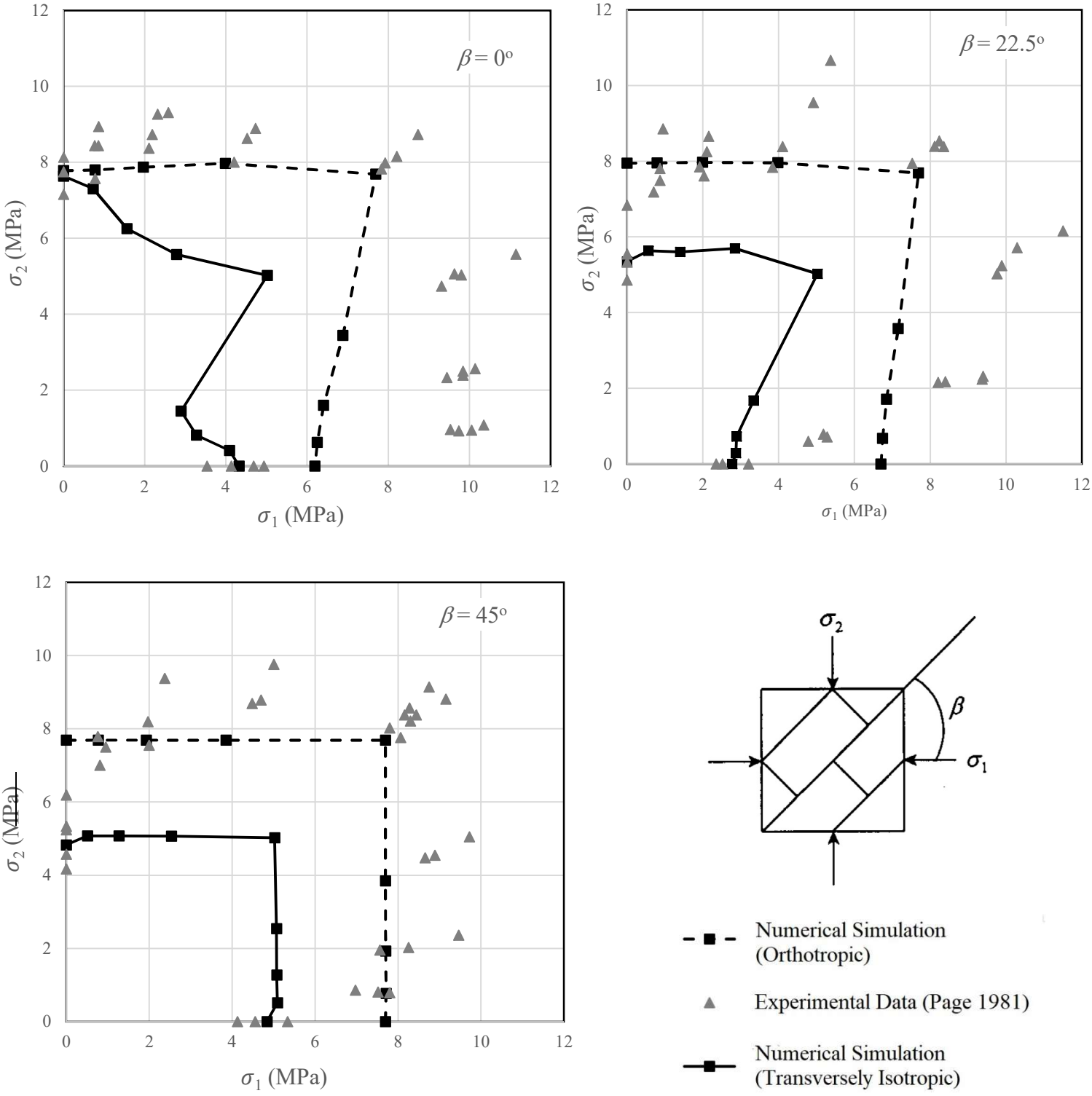

Figure 2.9 Failure Surfaces for In Plane Biaxial Compression Tests

CHAPTER 3

FINITE ELEMENT ANALYSIS OF A LARGE-SCALE MASONRY STRUCTURE

3.1. Introduction

This chapter discusses an application of the proposed macroscopic failure criterion in the numerical analysis. A 3D finite element simulation of a shaking table test is performed involving a reduced model of a building constructed with concrete and unreinforced masonry. In this simulation, the macroscopic failure criterion is incorporated for assessing the plastic admissibility of the stress field in the structure under earthquake excitation. The shaking table test was carried out at the Institute of Earthquake Engineering and Engineering Seismology (IEEES), Skopje (Jurukovski et al. 1989). The test involved a reduced 1:3 scale model of the building that was designed based on the Theory of Models and subjected to a specific earthquake excitation (Ushaksaraei et al., 2007).

The details of the 3D FE modelling of the shaking table tests are described in the following section. The dynamic FE analysis is performed within the elastic range, and the plastic

admissibility of the stress field is assessed by invoking the macroscopic failure criterion (2.1). The numerical results (the damaged zone at the peak displacement) are presented and compared with the crack pattern at the experimental test.

3.2. FE Simulation of the Reduced Scale Model Test

3.2.1 Geometry of the Model

Figure 3.1 shows the panel of the reduced scale model which was constructed on scale $1/3$ in relation to the size of the shaking table. This model includes RC (reinforced concrete) slabs, RC frame in the basement, and unreinforced masonry walls with 8 cm thickness. The size of masonry brick is $8 \times 8 \times 4$ cm. while the size of the panel is 410×350 cm.

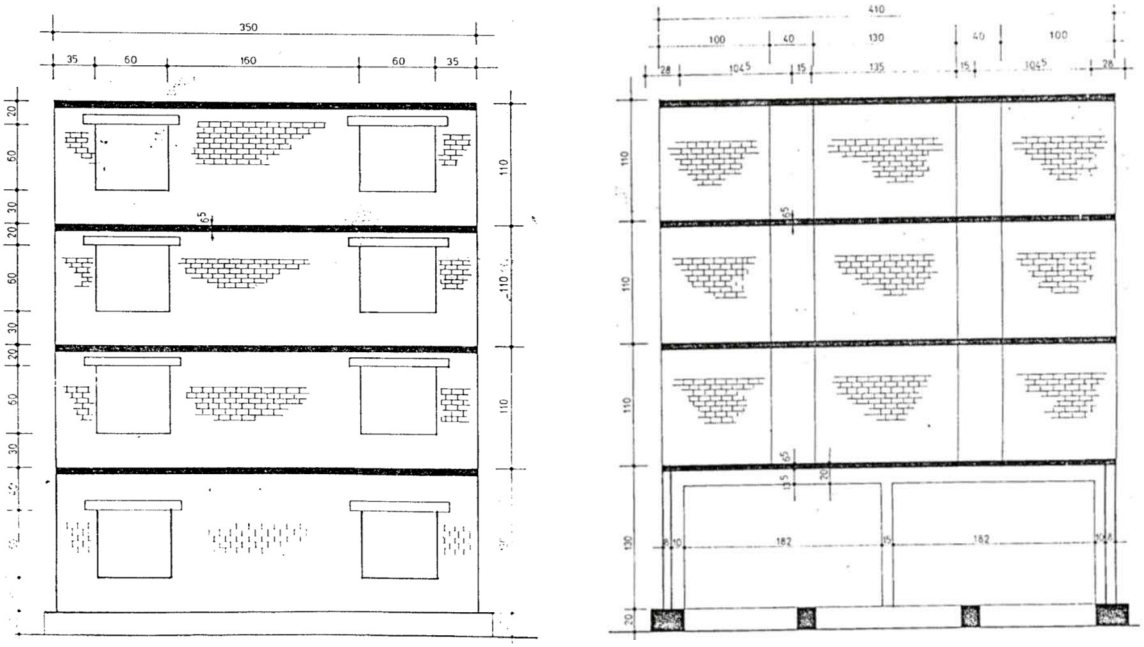

Figure 3.1 Reduced Scale Model Panel (Jurukovski et al. 1989)

3.2.2 Boundary Conditions and Discretization

Figure 3.2 shows the ground motion history used in the dynamic analysis. This base excitation is considered for each four directions, +x, –x, +z, –z, in the separate dynamic analyses. The maximum horizontal base acceleration was 0.5091g at 4.56 seconds.

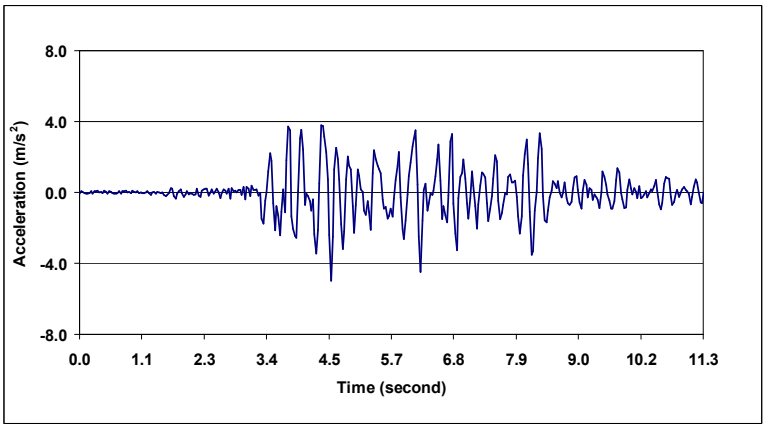

Figure 3.2 Base Acceleration History (R. Ushaksaraei et al. , 2007)

Figure 3.3 presents the FE discretization of the building. The 8-node linear hexahedral solid element type (C3D8) is employed in the finite element mesh for modeling the masonry walls, the concrete slabs, and the concrete beams above the window opening. A total of 9310 elements have been used.

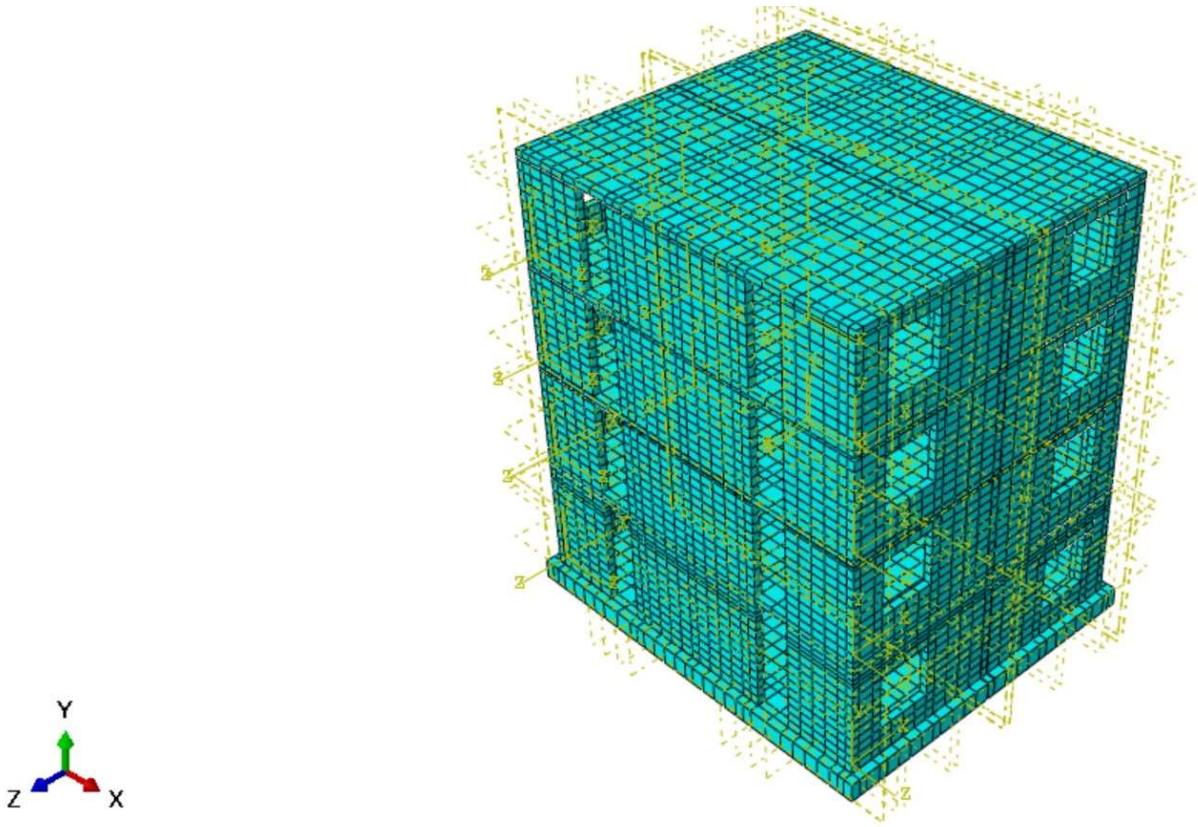

Figure 3.3 FE Discretization of the Mixed Concrete Masonry Building

3.2.3 Material Properties

The material properties for the constituents in this model have been provided by R. Ushaksaraei et al. (2007), Table 3.1. Also, the average elastic properties of the masonry brickwork have been computed through a general three-dimensional formulation developed by Pietruszczak and Niu (1992):

$$E_x = 1.5 \text{ GPa } E_y = 1.8 \text{ GPa } E_z = 1 \text{ GPa}$$
$$G_{xy} = 360 \text{ MPa } G_{yz} = 600 \text{ MPa } G_{xz} = 360 \text{ MPa}$$
$$\nu_{xy} = 0.14 \ \nu_{yz} = 0.24 \ \nu_{xz} = 0.24$$

Constituent	Property	Value
Brick	Angle of internal friction, ϕ (^{o})	55
	Cohesion, c (MPa)	2.38
	Tensile strength, σ_0 (MPa)	1.5
Mortar	Angle of internal friction, ϕ (^{o})	50
	Cohesion, c (MPa)	0.35
	Tensile strength, σ_0 (MPa)	0.15
Concrete	Density, γ (kg/m^3)	2400
	Module of Elasticity, E (GPa)	10.5
	Poisson' ratio, ν	0.2

Table 3.1 Material Properties of Constituents in Shaking Table Test Model (R. Ushaksaraei et al. 2007)

In order to implement the failure function in the numerical analysis, the material parameters should be specified for this case following the identification procedure described in Section 2.3. The material parameters associated with the spatial distribution of function $c(n_i)$, Equation (2.24), were derived by Ushaksaraei and Pietruszczak (2008). In this case, the variation of the uniaxial tensile strength has the form shown in Figure 3.4 and corresponds to the following parameters

$$c_0 = 0.33374 \quad \Omega_1 = 0.17853 \quad b_1 = -0.077 \quad b_2 = 3.46131$$

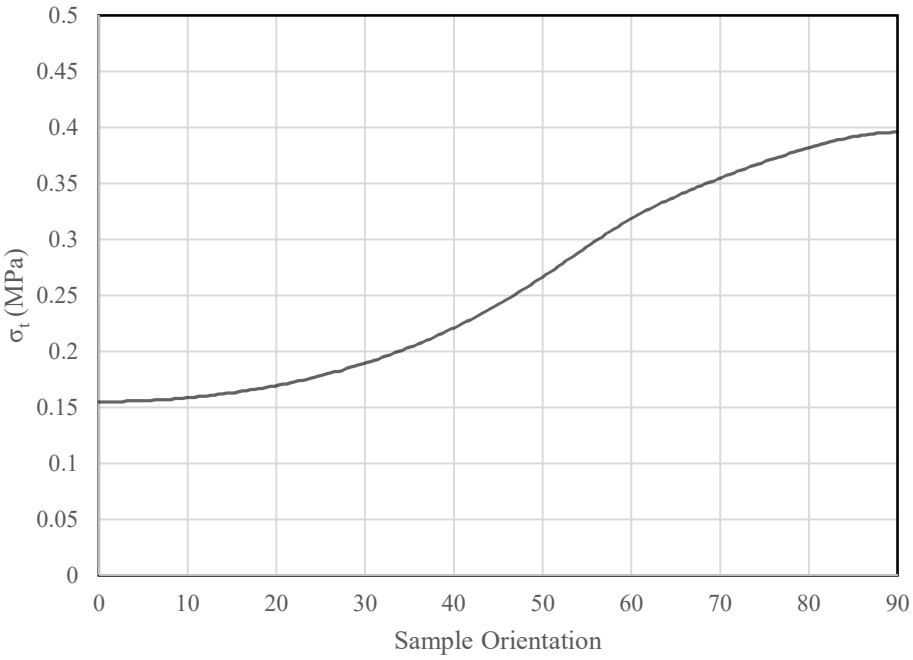

Figure 3.4 Uniaxial Tension Strength of Structural Masonry Variation for Shaking Table Test at IEEES Skopje (1989)

As stated in Section 2.3, the identification of the material function η_f, Equation 2.11, and the strength parameter C requires the uniaxial compression and the biaxial compression tension tests data for different orientations of bed joints. These data have been generated using the results based on Critical Plane approach as reported by Ushaksaraei and Pietruszczak (2008). The key values are presented in Table 3.8 below.

Bedding Angle β	Uniaxial Compressive, f_c (MPa)	Biaxial Compression Tension					
		$\alpha = 0.2$		$\alpha = 0.1$		$\alpha = 0.033$	
		σ_2(MPa)	σ_1(MPa)	σ_2(MPa)	σ_1(MPa)	σ_2(MPa)	σ_1(MPa)
0	4.343	1.579	0.315	2.491	0.249	0.983	0.327
22.5	1.932	1.105	0.221	1.420	0.142	0.860	0.286
45	3.442	1.465	0.293	2.235	0.223	0.871	0.290
67.5	4.081	0.997	0.199	2.035	0.203	0.586	0.195
90	1.888	0.774	0.154	1.482	0.148	0.466	0.155

Table 3.2 Uniaxial Compression and Biaxial Compression Tension Tests Data for Shaking Table Test at IEEES Skopje (1989)

By following now the identification procedure described in Chapter 2 and using the above set of data, the values of the parameter *C* and the approximation coefficients appearing in the function η_f have been determined as

$$\eta_f = 2.003 \quad A_1 = 0.119 \quad b_1 = -26.002 \quad b_2 = -84.229 \quad b_3 = 167.005 \quad C=0.83$$

Bedding Angle, β	$f_c(MPa)$	C		
		$\alpha = 0.2$	$\alpha = 0.1$	$\alpha = 0.033$
0.0	4.343	0.56	0.67	0.47
22.5	1.932	0.70	0.74	0.70
45.0	3.442	0.60	0.78	0.44
67.5	4.081	0.28	0.45	0.24
90.0	1.888	0.30	1.08	0.23
	Max	0.70	1.08	0.70
		C (Final)	0.83	

Table 3.3 Cohesion Parameter (C) for Shaking Table Test at IEEES Skopje (1989) for different bedding plane orientations

Bedding Angle, β	$f_c(MPa)$	C	ϕ	l_2	$1-3{l_2}^2$	η_f
0	4.343	0.830	0.809	1.000	-2.000	1.907
22.5	1.932	0.830	0.568	0.924	-1.561	1.311
45	3.442	0.830	0.740	0.707	-0.500	1.741
67.5	4.081	0.830	0.791	0.383	0.561	1.863
90	1.888	0.830	0.561	0.000	1.000	1.294

Table 3.4 Anisotropy Parameter η_f for Shaking Table Test at IEEES Skopje (1989) for different bedding plane orientations

3.3. Numerical Results and Discussion

In this section, the main results of the FE dynamic analysis of the masonry building, performed within the elastic range, are presented and the plastic admissibility of the resulting stress field is assessed.

Figure 3.5 shows the distribution of the value of the failure function, Equation (2.1), along the surfaces of the masonry walls at the peak displacement for the seismic excitation in the direction of +x. In this figure, the regions shown in red experience F>0, which means that the stress field is plastically inadmissible, i,e, the cracks will occur in the masonry brickwork. It is noted that the results only indicate the regions where the crack will form, the prediction of the crack pattern requires an appropriate non-linear analysis. The actual crack pattern recorded in the experimental test is depicted in Figure 3.6. In general, the predicted damage regions, Figure 3.5, are fairly consistent with the experimental results. The results for seismic excitation in other directions are presented in Figure 3.7.

Finally, the damaged regions in tension and compression are shown in Figures 3.8 (a) and (b), respectively. Comparing these two distributions, it is seen that the failure of the masonry brickwork, i.e., F>0, under seismic excitation happens mostly in the tension regime. This is due to the fact that the stress field in this regime violates the tension cut-off criterion based on the critical plane approach, Eq (2.20). At the same time, in compression regime the plastic admissibility is governed by the failure criterion incorporating microstructure tensor approach, Eq (2.14).

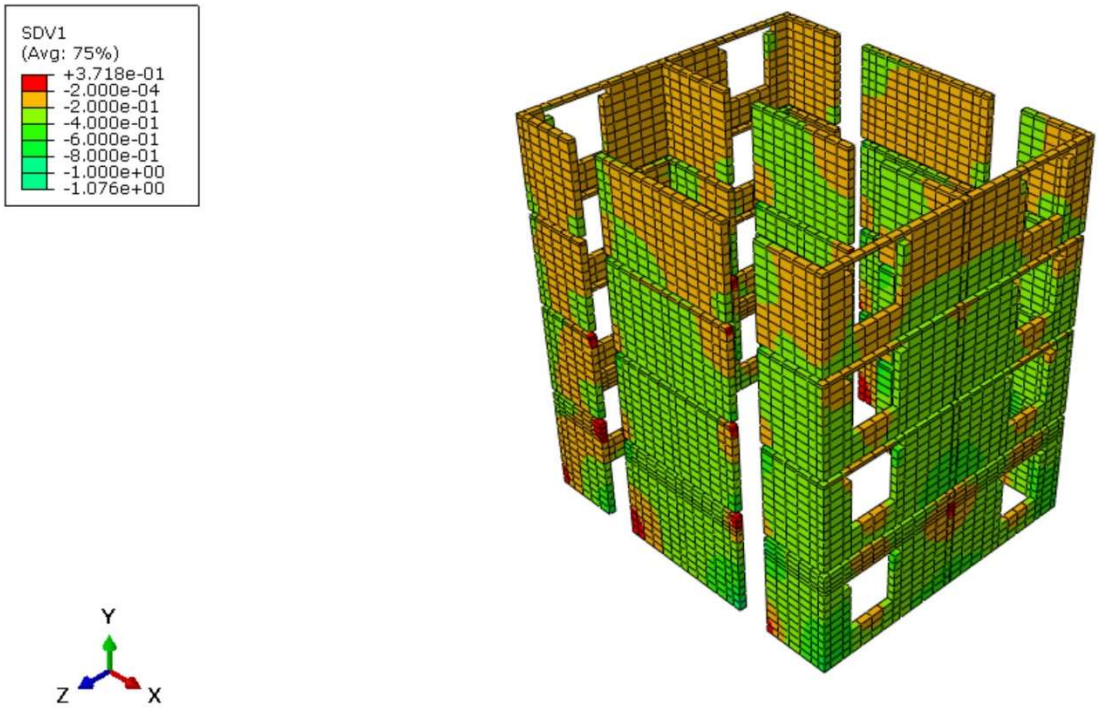
SDV1
(Avg: 75%)
+3.718e-01
-2.000e-04
-2.000e-01
-4.000e-01
-6.000e-01
-8.000e-01
-1.000e+00
-1.076e+00
Y
Z
X

a)

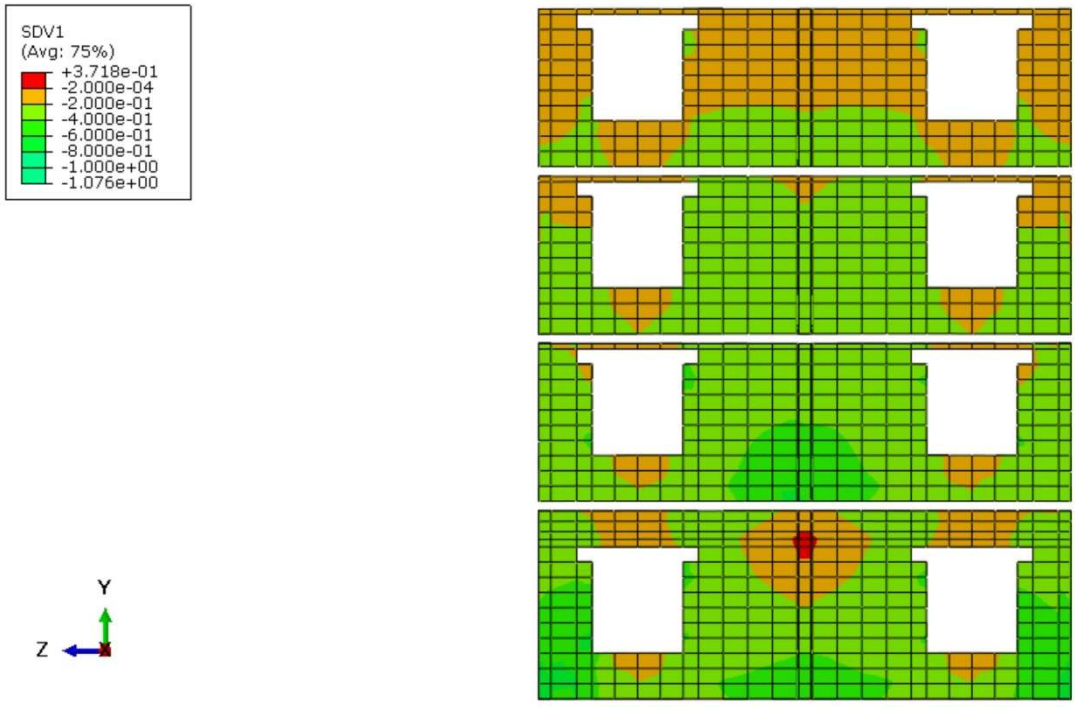
SDV1
(Avg: 75%)
+3.718e-01
-2.000e-04
-2.000e-01
-4.000e-01
-6.000e-01
-8.000e-01
-1.000e+00
-1.076e+00
Y
Z

b)

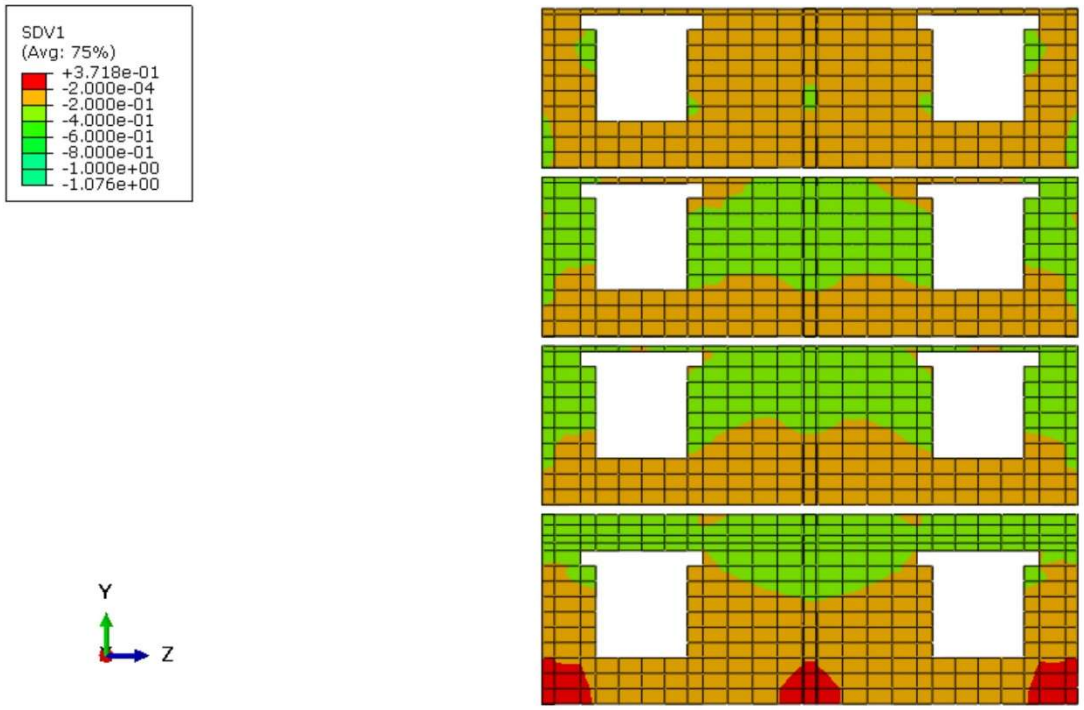
SDV1
(Avg: 75%)
+3.718e-01
-2.000e-04
-2.000e-01
-4.000e-01
-6.000e-01
-8.000e-01
-1.000e+00
-1.076e+00
Y
Z

c)

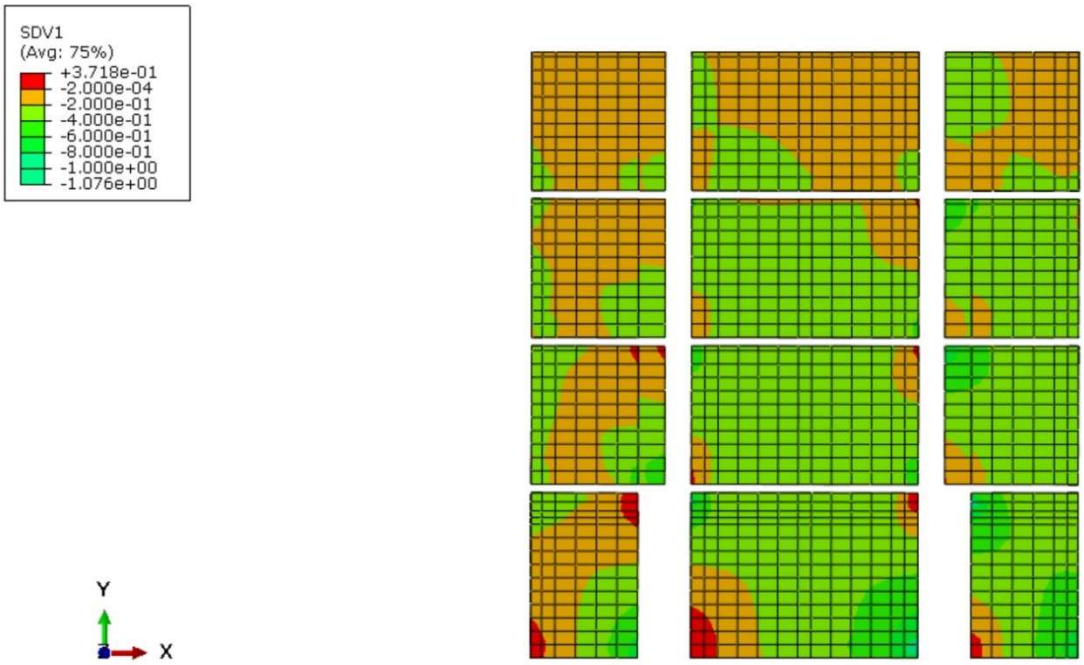
SDV1
(Avg: 75%)
+3.718e-01
-2.000e-04
-2.000e-01
-4.000e-01
-6.000e-01
-8.000e-01
-1.000e+00
-1.076e+00
Y
X

d)

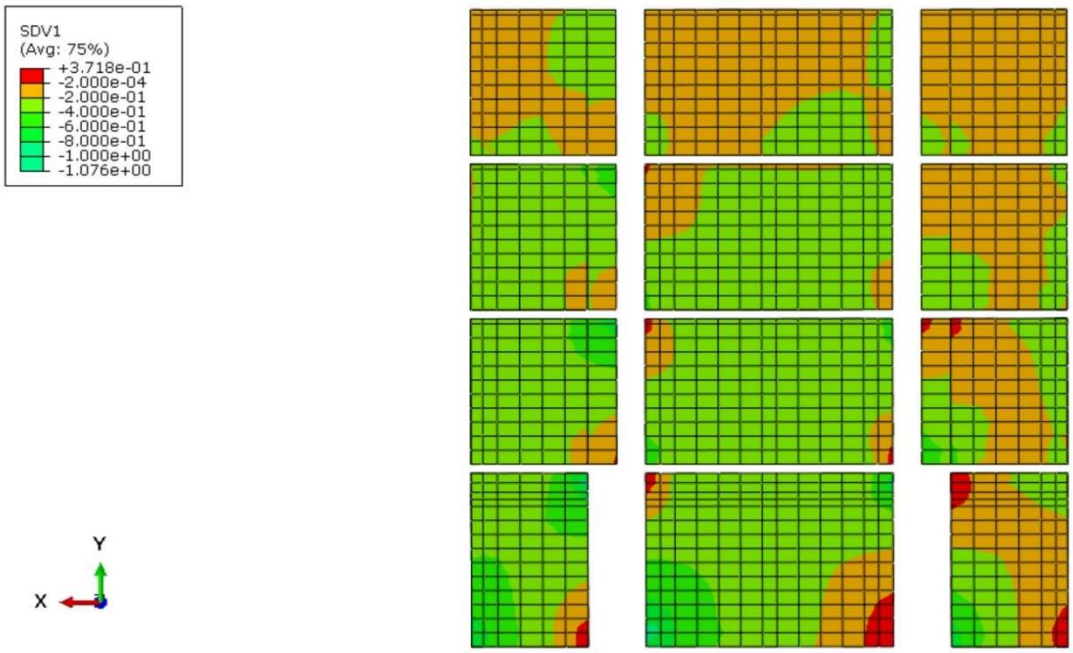

e)

Figure 3.5 Distribution of Failure Function of the Numerical Model for Maximum Base Acceleration in the Direction of +x a) 3D View b) Front Side c) Back Side d) Left Side e) Right Side

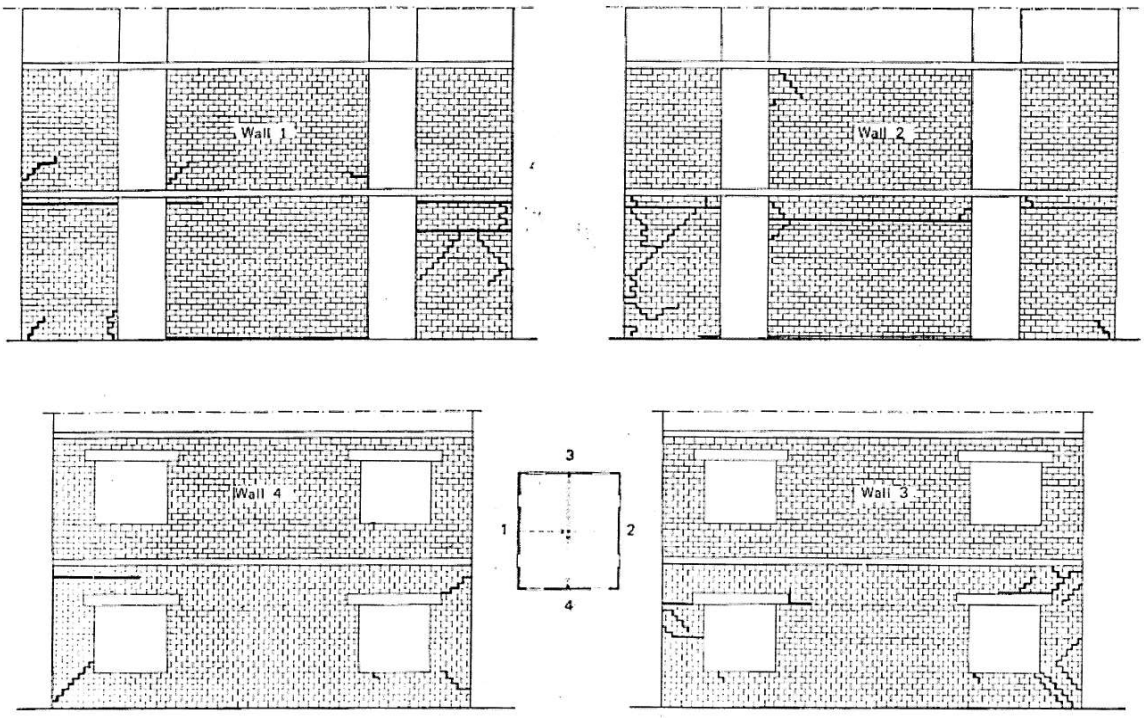

Figure 3.6 Crack Pattern of Masonry Walls in the Experimental Shaking Table Test, Front Side (Bottom Left), Back Side (Bottom Right), Left Side (Top Left), Right Side (Top Right) (Jurukovski et al. 1989)

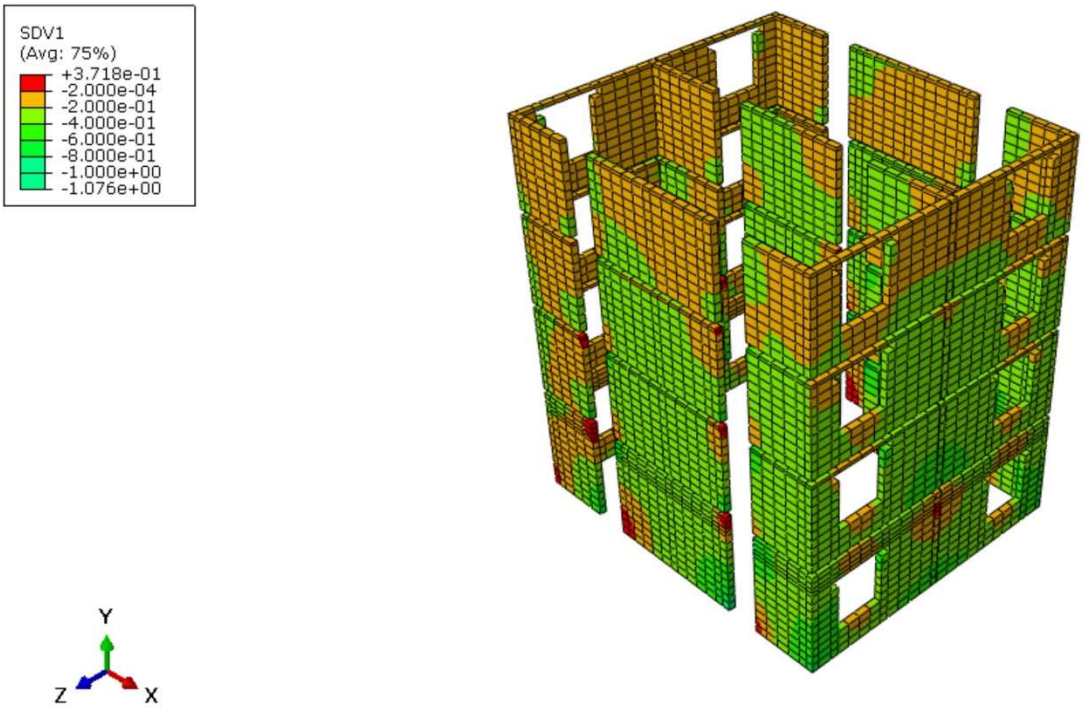
SDV1
(Avg: 75%)
+3.718e-01
-2.000e-04
-2.000e-01
-4.000e-01
-6.000e-01
-8.000e-01
-1.000e+00
-1.076e+00
Y
Z
X

a)

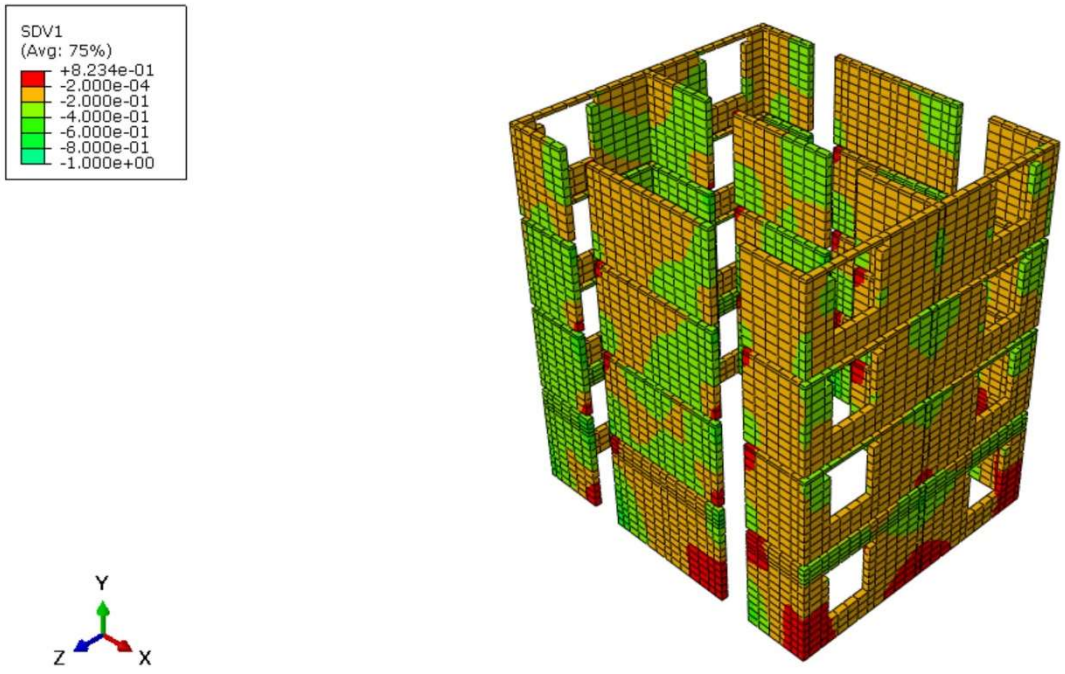
SDV1
(Avg: 75%)
+8.234e-01
-2.000e-04
-2.000e-01
-4.000e-01
-6.000e-01
-8.000e-01
-1.000e+00
Y
Z
X

b)

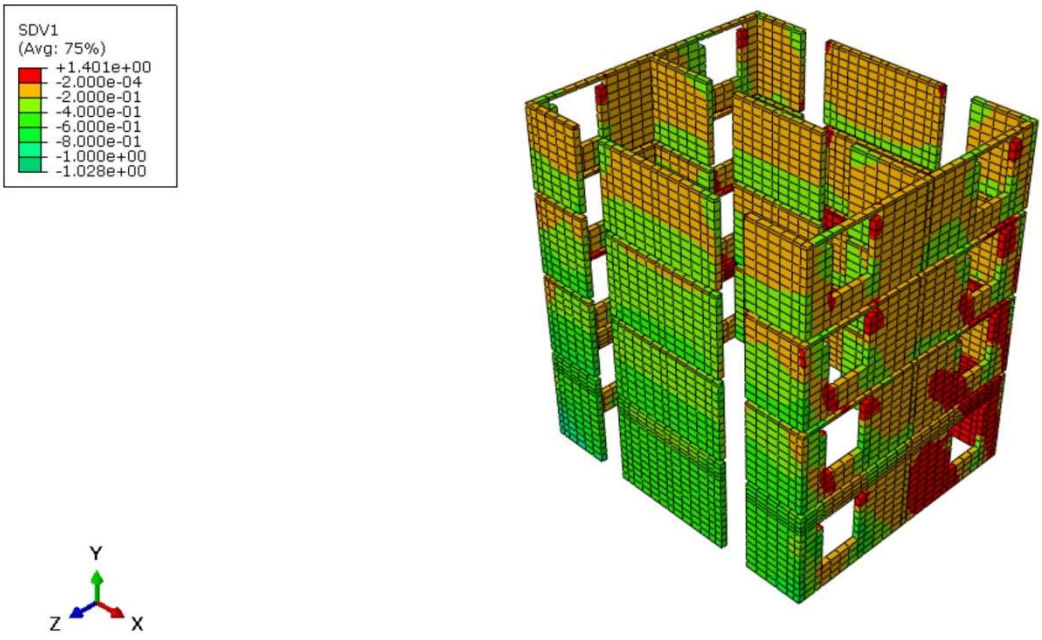

c)

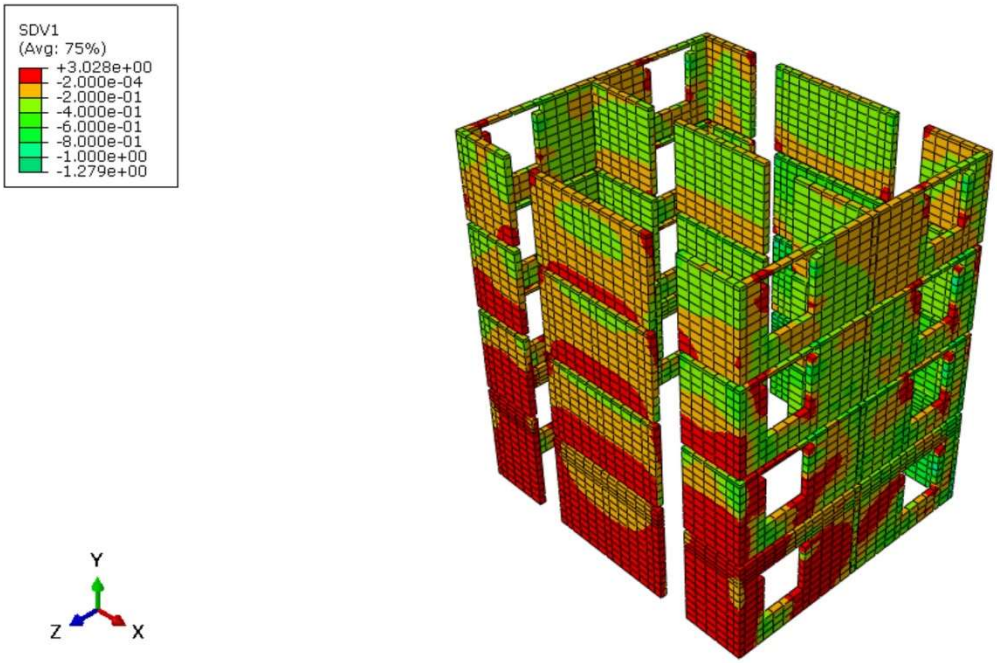

d)

Figure 3.7 Maps of Failure Function for Seismic Excitation in the Directions a) +x b) -x c) +z d) -z at the Maximum Displacement

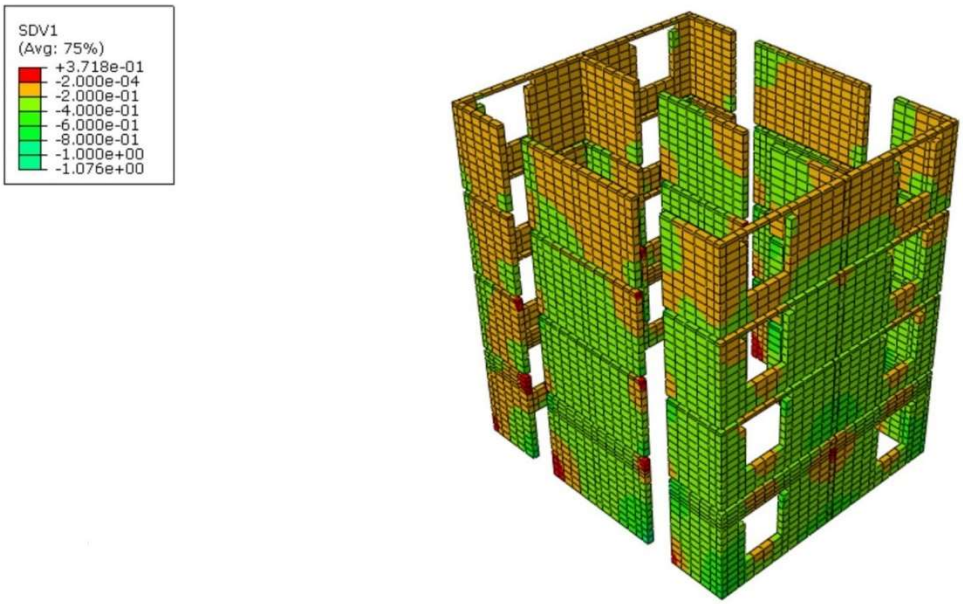

a)

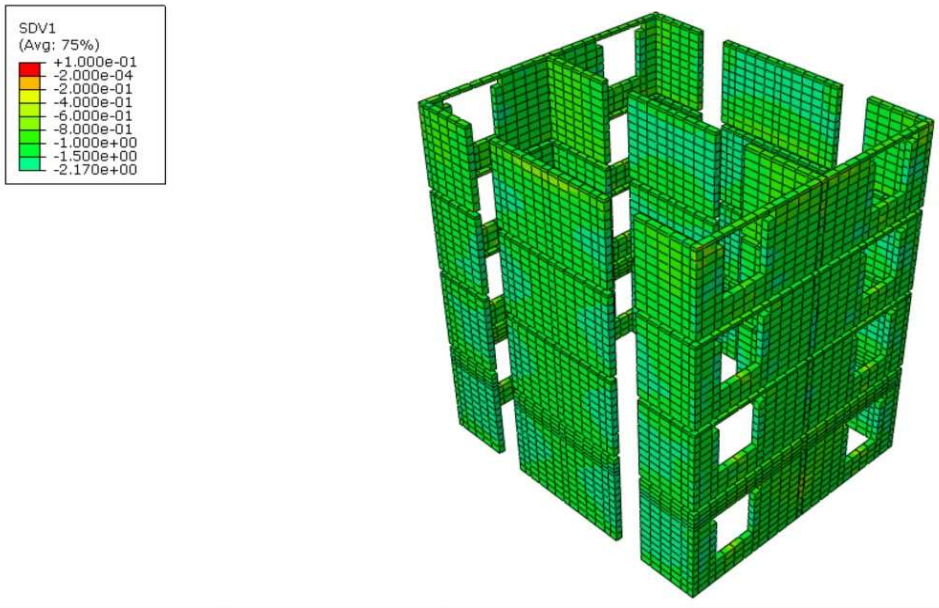

b)

Figure 3.8 Maps of Failure Function in a) Tension b) Compression Regimes, Seismic Excitation in the Direction of +x

Chapter 4

CONCLUSIONS AND FUTURE WORK

4.1. Summary and Conclusions

The analysis of structural masonry is difficult due to the complex mechanical behaviour of its constituents and their interaction. In Chapter 1, two main modeling approaches for masonry, i.e. meso-modelling and macro-modelling, have been reviewed. It was argued that the analysis of a real masonry structure should be performed by employing a macro-modelling approach in which the masonry brickwork is described by a representative element volume consisting of brick units with sets of mortar joints. Its average properties can be identified through different methods, such as homogenization approach, by considering the geometric arrangement of the constituents. In addition, in this approach, a macroscopic failure criterion is defined for the representative element to capture the failure condition of structural masonry. Two distinct approaches (Critical Plane Approach and Microstructure Tensor Approach) have been developed by Pietruszczak & Mroz (2001) to describe the anisotropy in material properties. In these approaches, a set of distribution functions are incorporated to define the spatial variation of strength. Ushaksaraei and Pietruszczak

(2002) derived a macroscopic constitutive model within the framework of the critical plane approach for structural masonry.

This study examined a macroscopic failure criterion for structural masonry which incorporates the microstructure tensor approach to specify the failure condition. This approach introduces a scalar anisotropy parameter, which is a function of mixed invariants of stress and microstructure-orientation tensors, to describe the anisotropic properties of brickwork. The framework incorporates an enhanced version of Mohr-Coulomb failure criterion for failure in compression regime, while in tension the conditions at failure are defined by employing the critical plane approach.

Using the experimental data provided by Page (1981,1983), material parameters/functions have been identified including strength descriptors associated with the failure condition, coefficients involved in the distribution functions of anisotropy parameter η_f and strength parameter c. Some simplified assumptions were incorporated in some parts of the identification process due to the lack of the experimental information.

The performance of the proposed macroscopic failure criterion has been verified through the numerical simulations of the experimental tests conducted by Page (1981&1983) including uniaxial tension, uniaxial compression, biaxial compression-tension, and biaxial compression-compression tests. The predicted results are consistent with the experimental data. Moreover, it was shown that the out-plane properties of masonry brickwork have a profound influence on the results of the in-plane biaxial compression-compression tests and the assumption of transverse isotropy is not valid in these tests.

In the final part of this study, a seismic analysis of a scaled four-storey masonry building was conducted by incorporating the macroscopic failure criterion into a user-defined material subroutine UMAT (Abaqus/Standard code). The analysis was performed within the elastic region. The numerical results include the maps of the failure function values along the outer faces at the peak base acceleration, indicating the damged zones. Comparing the predicted damage zones with the numerical simulation and the crack pattern in the experimental test, it was observed that they are fairly consistent with each other. Moreover, the results revealed that the failure in the masonry walls subjected to seismic loading occurs mostly in the tension regime.

4.2. Future Directions

In this study, a macroscopic criterion has been investigated for specifying the condition at failure in terms of the microstructure tensor for structural masonry. However, more studies are required to improve the performance of the proposed failure criterion. Therefore, some suggestions for future research are presented here.

The identification of material parameters requires some additional experimental studies, such as the direct shear tests and the triaxial compression test. The reason is that some material properties, such as the out-of-plane characteristics, which play an important role in the results of the compression tests, cannot be identified based on the information on the in-plane tests alone. Thus, numerical simulations of other experimental tests can be the subjects of further research.

The current approach based on the microstructure tensor describes the behaviour of the structural masonry within the elastic range, but it can be extended for modeling of progressive failure in the structural masonry by incorporating it within a plasticity framework. Such a

constitutive model will be capable of modeling the deformation characteristics in elastic as well as the elastoplastic range.

Finally, the Mohr-Coulomb failure criterion, which is incorporated in this project to describe the conditions at failure, is not able to capture the effect of the intermediate principal stress σ_{II}. The experimental data indicates that for the biaxial compression this stress component plays an important role in the failure condition. Therefore, it would be desirable to modify the Mohr-Coulomb failure criterion to consider the effect of the intermediate principal stress in order to adequately predict the behaviour of the structural masonry in compression regime.

References

Abaqus User Subroutines Reference Guide, Simulia Abaquus 6.14. https://www.sharcnet.ca/Software/Abaqus/6.14.2/v6.14/books/sub/default.htm?startat=ch02s01abu15.html

Andreaus U. 1996. “Failure Criteria for Masonry Panel under In-Plane Loading.” *Journal of Structural Engineering, ASCE* 122 (1): 37–46.

Anthoine, A. 1995. “Derivation of the In-Plane Elastic Characteristics of Masonry through Homogenization Theory.” *International Journal of Solids and Structures* 32 (2): 137–63. https://doi.org/10.1016/0020-7683(94)00140-R.

Anthoine, Armelle. 1997. “Homogenization of Periodic Masonry: Plane Stress, Generalized Plane Strain or 3D Modelling?” *Communications in Numerical Methods in Engineering* 13 (5): 319–26. https://doi.org/10.1002/(SICI)1099-0887(199705)13:5<319::AID-CNM55>3.0.CO;2-S.

Atkinson, R.H., Noland, J.L., Abrams, D.P., and McNary, S. 1985. “A Deformation Failure Theory for Stack-Bond Brick Masonry Prisms in CompressionTitle.” In *Proceedings of the Third North American Masonry Conference*, 577–92.

Bierwirth, H., Sto ̈ckl, S., and Kupfer, H. 1993. “Triaxial Tests on Mortar Specimens Taken from Bed Joints.” In *6th North American Masonry Conference*, 995–1007. Drexel University, Philadelphia, Pennsylvania, USA.

Boehler, J., & Sawczuk, A. 1970. “Equilibre Limite Des Sols Anisotropes.” *J. Mécanique* 9: 5–33.

Cowin, Stephen C. 1986. “Fabric Dependence of an Anisotropic Strength Criterion.” *Mechanics of Materials* 5 (3): 251–60. https://doi.org/10.1016/0167-6636(86)90022-0.

Drysdale, RG., and Khattab, M.M. 1995. “In-Plane Behavior of Grouted Concrete Masonry under Biaxial Tension-Compression.” *ACI Struct. J* 92 (6): 653–64.

Duveau, G., J. F. Shao, and J. P. Henry. 1998. “Assessment of Some Failure Criteria for Strongly Anisotropic Geomaterials.” *Mechanics of Cohesive-Frictional Materials* 3 (1): 1–26. https://doi.org/10.1002/(SICI)1099-1484(199801)3:1<1::AID-CFM38>3.0.CO;2-7.

Hill, R. 1948. “A Theory of the Yielding and Plastic Flow of Anisotropic Metals.” *Proceedings of the Royal Society A: Mathematical, Physical and Engineering Sciences* 193 (1033): 281–97. https://doi.org/10.1098/rspa.1948.0045.

Hoek, Evert. 1964. “Fracture of Anisotropic Rock.” *Journal of the South African Institute of Mining and Metallurgy* 64 (10): 501–18.

J. C. Jaeger. 1960. “Shear Failure of Anisotropic Rocks.” *Geological Magazine* 97 (1): 65–72.

Jurukovski D., Tashkov Lj., Petkovski M. & Mamucevski D. 1989. “Basic and Applied Research Study for Seismic Modeling of Mixed Reinforced Concrete Masonry Buildings.”

Lourenco, P.B., Rots, J.G., and Blaauwendraad, J. 1994. “Implementation of an Interface Cap Model for the Analysis of Masonry Structures.” In *Computational Modelling of Concrete Structures,Pineridge Press, Swansea,* 123–34.

Lourenco, P.B. and Rots, J.G. 1993. “On the Use of Micro-Models for the Analysis of Masonry Shear-Walls.” In *Computer Methods in Structural Masonry - 2,* 14–26. Swansea, UK,.

Lourenco, Paulo B., Jan G. Rots, and Johan Blaauwendraad. 1998. “CONTINUUM MODEL FOR MASONRY: PARAMETER ESTIMATION AND VALIDATION By Paulo B.” *Journal of Structural Engineering, ASCE* 124 (6): 642–52.

Ma, G., Hao, H., and Lu, Y. 2001. “Homogenization of Masonry Using Numerical Simulations.” *Journal of Engineering Mechanics. ASCE,* 127 (5): 421–31.

Masiani, R, and P Trovalusci. 1996. “Cauchy and Cosserat Materials as Continuum Models of Brick Masonry.” *Meccanica* 31 (4): 421–32.

McLamore, R., & Gray, K. E. 1967. “The Mechanical Behavior of Anisotropic Sedimentary Roks.” *Journal of Engineering for Industry* 89 (1): 62–73.

Page, A.W. 1978. “Finite Element Model for Masonry.” *J Struct. Div., ASCE* 104 (8): 1267–85.

Page, A.W. 1981. “The Biaxial Compressive Strength of Brick Masonry.” *Proceedings of the Institution of Civil Engineers* 71 (3): 893–906. https://doi.org/10.1680/iicep.1981.1825.

Page, A.W. 1983. “The Strength of Brick Masonry under Biaxial Tension-Compression.” *Int. J Masonry Constr* 3 (1): 26–31.

Pande, G.N., Liang, lX., and Middleton, J. 1989. “Equivalent Elastic Moduli for Brick Masonry.” *Computers and Geotechnics* 8: 243–65.

Pariseau, W. G. 1968. “Plasticity Theory For Anisotropic Rocks And Soil. American Rock Mechanics Association.” In *In The 10th US Symposium on Rock Mechanics (USRMS).*

American Rock Mechanics Association.

Paulo B. Lourenco, and Jan G. Rots. 1997. "Multisurface Interface Model for Analysis" 123 (7): 660–68.

Pietruszczak, S. 2010. *Fundamentals of Plasticity in Geomechanics*. CRC Press. CRC Press. https://books.google.ca/books?id=_WsVQwAACAAJ&dq=pietruszczak,+S.+2010.+Fundamentals+of+Plasticity+in+Geomechanics.+CRC+Press.+CRC+Press.&hl=en&sa=X&ved=0ahUKEwjV2OPtyN7dAhUB6IMKHf2TDMgQ6AEIPTAE

Pietruszczak, S., and E. Haghighat. 2015. "Modeling of Deformation and Localized Failure in Anisotropic Rocks." *International Journal of Solids and Structures* 67–68: 93–101. https://doi.org/10.1016/j.ijsolstr.2015.04.004.

Pietruszczak, S., and Z. Mroz. 2001. "On Failure Criteria for Anisotropic Cohesive-Frictional Materials." *International Journal for Numerical and Analytical Methods in Geomechanics* 25 (5): 509–24. https://doi.org/10.1002/nag.141.

Pietruszczak, S, and X Niu. 1992. "A Mathematical Description of Macroscopic Behavior of Unit Masonry." *International Journal of Solids and Structures* 29 (5): 531–46.

Piszczek, K., Szarlinski, J. and Urbanski, A. 2001. "Identification of Orthotropic Mechanical Properties of Brick Masonry by an Homogenization Technique." *Computer Methods in Structural Masonry - 5, Computers & Geotechnics Ltd, Swansea,* 52–59.

R. Ushaksaraei, S. Pietruszczak, Gocevski, V. 2007. "Critical Plane Approach; Application to Seismic Analysis of Masonry Structures." In *10th, International Symposium on Numerical Models in Geomechanics; Numerical Models in Geomechanics*, 685–90. Rhodes, Greece.

Raffard, D., P. Ienny, J. P. Henry, and F. Homand. 2001. “Masonry: Stone/Mortar Interface Behaviour Characterization by Optical Extensometer.” *Mechanics Research Communications* 28 (1): 33–40. https://doi.org/10.1016/S0093-6413(01)00141-0.

Samarasinghe, W., and Hendry, A.W. n.d. “Strength of Brickwork Under Biaxial Tensile and Compressive Stress.” In *The British Ceramic Society, Load Bearing Brickwork*, 129–39.

Shieh-Beygi, B., and S. Pietruszczak. 2008. “Numerical Analysis of Structural Masonry: Mesoscale Approach.” *Computers and Structures* 86 (21–22): 1958–73. https://doi.org/10.1016/j.compstruc.2008.05.007.

Sulem, J., and Hans-B Muhlhaus. 1997. “A Continuum Model for Periodic Two-Dimensional Block Structures.” *Mechanics of Cohesive-Frictional Materials* 2: 31–46. https://doi.org/10.1002/(SICI)1099-1484(199701)2:1<31::AID-CFM24>3.0.CO;2-O.

Tsai, S. W., & Wu, E. M. 1971. “A General Theory of Strength for Anisotropic Materials.” *Journal of Composite Materials* 5(1): 58–80.

Ushaksaraei, R., and S. Pietruszczak. 2002. “Failure Criterion for Structural Masonry Based on Critical Plane Approach.” *Journal of Engineering Mechanics* 128 (7): 769–78. https://doi.org/10.1061/(ASCE)0733-9399(2002)128:7(769).